AMERICAN SOCIETY FOR MICROBIOLOGY | mBio®

RESEARCH ARTICLE

Protein Prenylation and Hsp40 in Thermotolerance of *Plasmodium falciparum* Malaria Parasites

Emily S. Mathews,[a] Andrew J. Jezewski,[a,b] Audrey R. Odom John[a,c,d]

[a]Department of Pediatrics, Washington University School of Medicine, St. Louis, Missouri, USA
[b]Department of Pediatrics, Carver College of Medicine, University of Iowa, Iowa City, Iowa, USA
[c]Department of Molecular Microbiology, Washington University School of Medicine, St. Louis, Missouri, USA
[d]Division of Infectious Disease, Department of Pediatrics, Children's Hospital of Philadelphia, Perelman School of Medicine, University of Pennsylvania, Philadelphia, Pennsylvania, USA

ABSTRACT During its complex life cycle, the malaria parasite survives dramatic environmental stresses, including large temperature shifts. Protein prenylation is required during asexual replication of *Plasmodium falciparum*, and the canonical heat shock protein 40 protein (HSP40; PF3D7_1437900) is posttranslationally modified with a 15-carbon farnesyl isoprenyl group. In other organisms, farnesylation of Hsp40 orthologs controls their localization and function in resisting environmental stress. In this work, we find that plastidial isopentenyl pyrophosphate (IPP) synthesis and protein farnesylation are required for malaria parasite survival after cold and heat shock. Furthermore, loss of HSP40 farnesylation alters its membrane attachment and interaction with proteins in essential pathways in the parasite. Together, this work reveals that farnesylation is essential for parasite survival during temperature stress. Farnesylation of HSP40 may promote thermotolerance by guiding distinct chaperone-client protein interactions.

KEYWORDS *Plasmodium falciparum*, farnesylation, heat shock, isoprenoids, malaria, protein chaperone

Infection with the protozoan parasite *Plasmodium falciparum* causes the majority of cases of severe and fatal malaria. *P. falciparum* must recognize and adapt to dramatic environmental stresses, as its complex life cycle requires development in both an invertebrate mosquito vector and the warm-blooded vertebrate human host. In particular, temperature is critical at every stage of the parasite life cycle. In the mosquito vector, many temperature-sensitive factors contribute to human transmission, such as biting rate, vector longevity, parasite development, and vector competence (1). Human infection begins upon the bloodmeal of a female *Anopheles* mosquito. Entering the human host, where the normal physiological temperature is 37°C, sporozoite-stage parasites experience heat shock. However, this temperature stress is necessary for efficient hepatocyte infection and the resulting amplification of infection (2, 3). The parasite emerges from the liver to initiate asexual replication within erythrocytes, the clinically symptomatic stage of *Plasmodium* infection. A pathognomonic feature of falciparum malaria is periodic episodes of fever (to 41°C or more) recurring every 48 h, corresponding to the synchronous rupture of infected erythrocytes and daughter merozoite release (4). In contrast, the sexual-stage parasites that return to the mosquito vector are again exposed to cold temperature shock, as the parasite must now readjust to approximately 25°C. While temperature fluctuations are an inherent part of the malaria life cycle, how the parasite copes with thermal stress is not well understood.

Temperature regulates both malaria pathogenesis and antimalarial sensitivity. Controlled hypothermia (32°C) has been used clinically to improve outcomes of severe cerebral malaria (5). *In vitro*, hypothermia (32°C) inhibits *P. falciparum* growth (6), and a similar effect occurs at

Citation Mathews ES, Jezewski AJ, Odom John AR. 2021. Protein prenylation and Hsp40 in thermotolerance of *Plasmodium falciparum* malaria parasites. mBio 12:e00760-21. https://doi.org/10.1128/mBio.00760-21.

Editor L. David Sibley, Washington University School of Medicine

Address correspondence to Audrey R. Odom John, johna3@email.chop.edu.

Received 15 March 2021
Accepted 1 June 2021
Published 29 June 2021

lower temperatures (28°C) (7). While the potency of some antimalarials (e.g., chloroquine, mefloquine, and pyronaridine) are unaffected by lower temperatures (6, 8), susceptibility to artemisinin—the backbone of front-line artemisinin-based combination therapies—is modulated by both cold and heat stresses (6, 8). As temperature fluctuations are an inherent part of the *P. falciparum* life cycle, this common environmental stress may affect the ability of antimalarials to influence essential parasite targets. Antimalarial resistance threatens malaria control efforts worldwide. In particular, rising rates of delayed clearance to artemisinin-based combination therapies, including resistance to artemisinin partner drugs, has raised concerns about emerging multidrug resistance (9–17). Thus, there is a pressing need to identify essential survival pathways in *P. falciparum*, such as thermotolerance, in order to support ongoing development of new antimalarial agents.

During intraerythrocytic development, *P. falciparum* assembles isoprenoids *de novo* through the methylerythritol 4-phosphate (MEP) pathway (18–20), localized within the unusual plastidial organelle of the parasite, the apicoplast. Chemical inhibition of this pathway by the small molecule fosmidomycin (FSM) is lethal to malaria parasites (18). FSM-mediated growth inhibition can be rescued by supplementation with isoprenoids such as isopentenyl pyrophosphate (IPP) (21, 22). These studies validate the essentiality of isoprenoid synthesis in asexual *P. falciparum*, but there have been long-standing questions regarding which biological processes in the parasite require apicoplast isoprenoid biosynthesis. Protein prenylation appears to be a core essential function of isoprenoid biosynthesis in malaria parasites (23–27). During protein prenylation, either a farnesyl (FPP; 15-carbon) or a geranylgeranyl (GGPP; 20-carbon) isoprenyl group is posttranslationally attached to C-terminal cysteines by one of three well-characterized prenyltransferases, farnesyltransferase (FTase) and geranylgeranyltransferases type I and type II (GGTase I, GGTase II). Chemical inhibition of prenyltransferases with small molecules (e.g., FTase inhibitor FTI-277) inhibits parasite growth (24–29), providing compelling evidence that prenylated malarial proteins and their unidentified downstream biological processes include potential antimalarial targets. We and others have used chemical labeling to characterize the complete prenylated proteome of intraerythrocytic *P. falciparum* (30, 31). These studies identify a single heat shock protein 40 (HSP40; PF3D7_1437900) as robustly farnesylated during intraerythrocytic replication.

Heat shock proteins are necessary for protein folding and stabilization. Importantly, heat shock proteins play a vital role in surviving cellular stresses that might otherwise be lethal, and therefore heat shock protein expression is upregulated under diverse cellular insults, including heat and cold shock. The main functions of Hsp40 family members are to identify and bind partially misfolded proteins in order to initiate Hsp70-mediated refolding. Inhibition of Hsp70 in *P. falciparum* was recently shown to hypersensitize parasites to heat shock conditions (32). As heat shock proteins have a known role in temperature-dependent survival, it is perhaps unsurprising that roughly 2% of the *P. falciparum* genome is dedicated to molecular chaperones, including a large number of heat shock proteins (33). HSP40 is a member of an expanded Hsp40 family in *P. falciparum* comprising 49 total members (34). The majority of Hsp40 family members in *P. falciparum* are unique and not shared with other Apicomplexa (34, 35). HSP40 is predicted to be the only canonical Hsp40 and the main cochaperone of Hsp70 in *P. falciparum* because of its similar heat inducibility and localization (36). The lack of additional canonical Hsp40s in *P. falciparum* suggests that HSP40 is necessary for parasite development. Critically, HSP40 is the sole prenylated heat shock protein in *P. falciparum* (30, 31). In yeast, prenylation of the HSP40 homolog YDJ1 is required for thermotolerance, protein localization, and interaction with client proteins (37–39). In *P. falciparum*, the role of farnesylated HSP40 (farnesyl-HSP40) has not previously been investigated.

In this study, we investigate the role of the apicoplast MEP pathway of isoprenoid biosynthesis and downstream protein prenylation on survival during environmental stress in *P. falciparum*. We find that plastidial IPP production is critical to parasite survival following either heat (40°C) or cold shock (25°C). In addition, we find that farnesylation, but not geranylgeranylation, is required for thermotolerance in *P. falciparum*. We also demonstrate that

the farnesylated heat shock protein HSP40 is likely essential. Farnesylation of HSP40 mediates its membrane association and directs its interaction with proteins in essential pathways in the parasite. Our work suggests HSP40 prenylation as a compelling candidate for a downstream effector by which IPP synthesis and protein farnesylation contribute to parasite stress survival.

RESULTS

Thermotolerance in malaria parasites requires IPP synthesis and protein farnesylation. The malaria parasite must adapt to diverse environmental stresses, such as large temperature shifts, throughout its complex life cycle. Heat shock proteins play an important role in the ability of the parasite to survive temperature stress (40–43). Because *P. falciparum* expresses a farnesylated heat shock protein, HSP40, we hypothesized that production of isoprenoids and protein prenylation are required for growth during temperature stress. We tested this hypothesis by inhibiting protein prenylation and applying either heat or cold stress.

Chemically diverse small molecule inhibitors affect protein prenylation during asexual replication of *Plasmodium* spp. For example, treatment with FSM, which inhibits upstream isoprenoid biosynthesis and therefore synthesis of prenylphosphates, reduces downstream protein prenylation (23). Well-validated prenyltransferase inhibitors, such as FTI-277 (FTI), BMS-388891 (BMS), and GGTI-298 (GGTI), directly reduce levels of protein prenylation in *P. falciparum* (28, 44) (Fig. 1A). We tested whether inhibition of prenylphosphate synthesis or prenyltransferases influenced parasite growth following heat (40°C) or cold (25°C) stress. These temperatures were selected to emulate temperatures in which the parasite is exposed during febrile episodes (for heat stress) and during transmission to the mosquito vector (for cold stress). Parasites were pretreated with inhibitor 24 h prior to temperature shock. Parasite growth was evaluated by flow cytometry (Fig. S1) for 6 days postshock (Fig. 1B).

While untreated parasites readily recovered following brief heat or cold shock (Fig. 1C and D), we found that parasite survival under heat (Fig. 1C) or cold (Fig. 1D) stress was significantly attenuated upon nonlethal inhibition of IPP synthesis by FSM. FTI and BMS are chemically unrelated, well-validated protein farnesyltransferase inhibitors, while GGTI inhibits protein geranylgeranylation. Using these inhibitors, we found that chemical inhibition of protein farnesylation, but not geranylgeranylation, significantly impaired temperature stress recovery (Fig. 1E; Fig. S2).

Taking advantage of the fact that FSM inhibits production of all isoprenoid products downstream of IPP, we employed chemical supplementation in order to determine which isoprenoids are required for temperature stress survival in malaria parasites. We found that supplementation with IPP or farnesol (F-OL), a 15-carbon farnesyl alcohol, rescued FSM-treated parasites after both heat and cold stress (Fig. 2B to D and F to H). In contrast, supplementation with geranylgeraniol (GG-OL), a 20-carbon geranylgeranyl alcohol, did not rescue growth of FSM-treated parasites after temperature shock (Fig. 2E and I). Altogether, these data establish that loss of isoprenoid biosynthesis or protein farnesylation sensitizes malaria parasites to changes in temperature. Protein farnesylation is thus required for parasite survival following moderate, nonlethal temperature stress, in which heat shock proteins have a classic biological role. Only 4 farnesylated proteins have been identified in *P. falciparum*, 2 SNARE proteins (PF3D7_1324700, PF3D7_0910600), a PI3P binding protein (PF3D7_1460100), and the sole canonical HSP40 (PF3D7_1437900) (30, 31). Since HSP40 is predicted to modulate the activity of HSP70, a cellular chaperone required for heat survival (32), these data raise the possibility that farnesylation of HSP40 might have a vital role in parasite thermotolerance.

HSP40 is resistant to disruption in *P. falciparum*. We next examined the specific role of HSP40 in asexual parasite growth. HSP40 is one member of an expanded Hsp40 chaperone family in *P. falciparum*. While the majority of these Hsp40 family members do not have assigned biological functions, HSP40 is considered the canonical member of this family and directly interacts with HSP70 (PF3D7_0818900) (36). Based on forward genetic screening in *P. falciparum*, HSP40 is predicted to be essential during

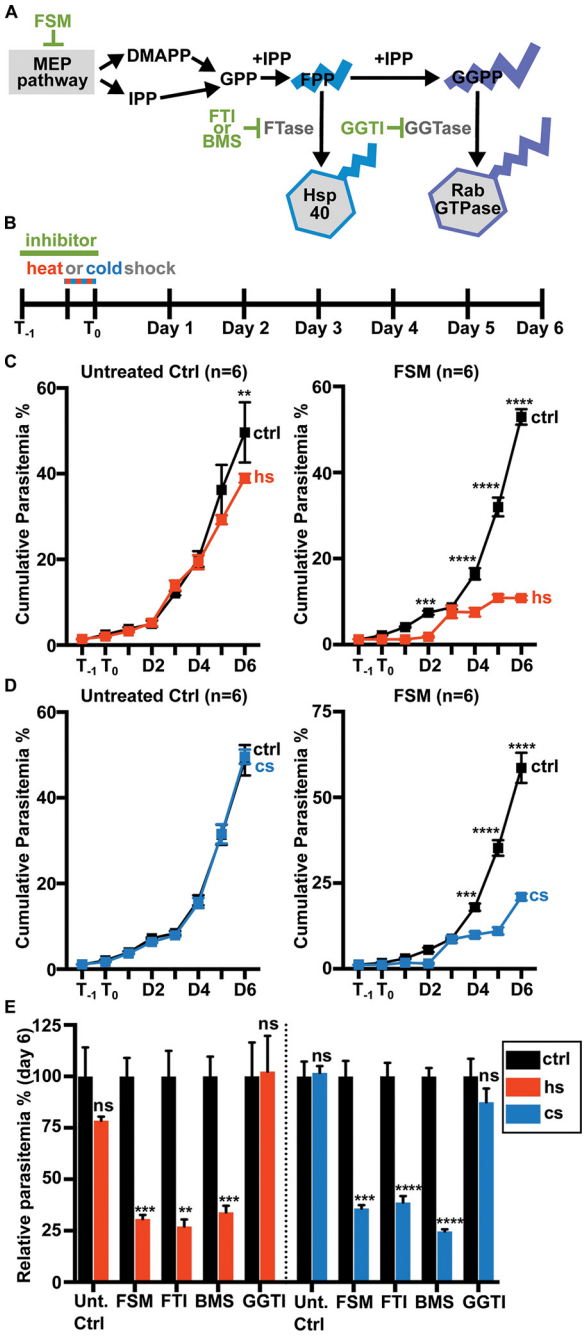

FIG 1 Growth under temperature stress requires IPP synthesis and protein farnesylation. (A) Prenylphosphate substrates for protein prenylation are derived from the nonmevalonate MEP pathway. MEP pathway products, IPP and dimethylallyl pyrophosphate (DMAPP), serve as precursors to FPP used by FTase and GGPP used by GGTase in protein prenylation. FSM treatment inhibits production of IPP and DMAPP. Farnesyltransferase inhibitors (FTI or BMS) inhibit protein farnesylation, while geranylgeranyltransferase inhibitors (GGTI) prevent protein geranylgeranylation. (B) Parasites were treated with FSM (5 μM), farnesyltransferase inhibitors (FTI [10 μM] and BMS [200 nM]), or geranylgeranyltransferase inhibitor GGTI (2 μM) for 24 h prior to a 6-h heat (40°C) or cold (25°C) shock. (C and D) FSM-treated parasite growth is significantly reduced after heat shock (C) and cold shock (D). (E) Inhibition of farnesylation by treating parasites with FTI or BMS significantly reduced growth after temperature stress. Growth in GGTI-treated parasites is unchanged after heat or cold shock. (C to E) $n = 6$; **, $P \leq 0.01$; ***, $P \leq 0.001$; ****, $P \leq 0.0001$. (C and D) 2-way ANOVA, P values adjusted for multiple comparisons using Sidak's multiple-comparison test. (E) Within each treatment group, the normalized control was compared to temperature shock sample by unpaired t test with Welch's correction. Abbreviations: ctrl, control, hs, heat shock, cs, cold shock.

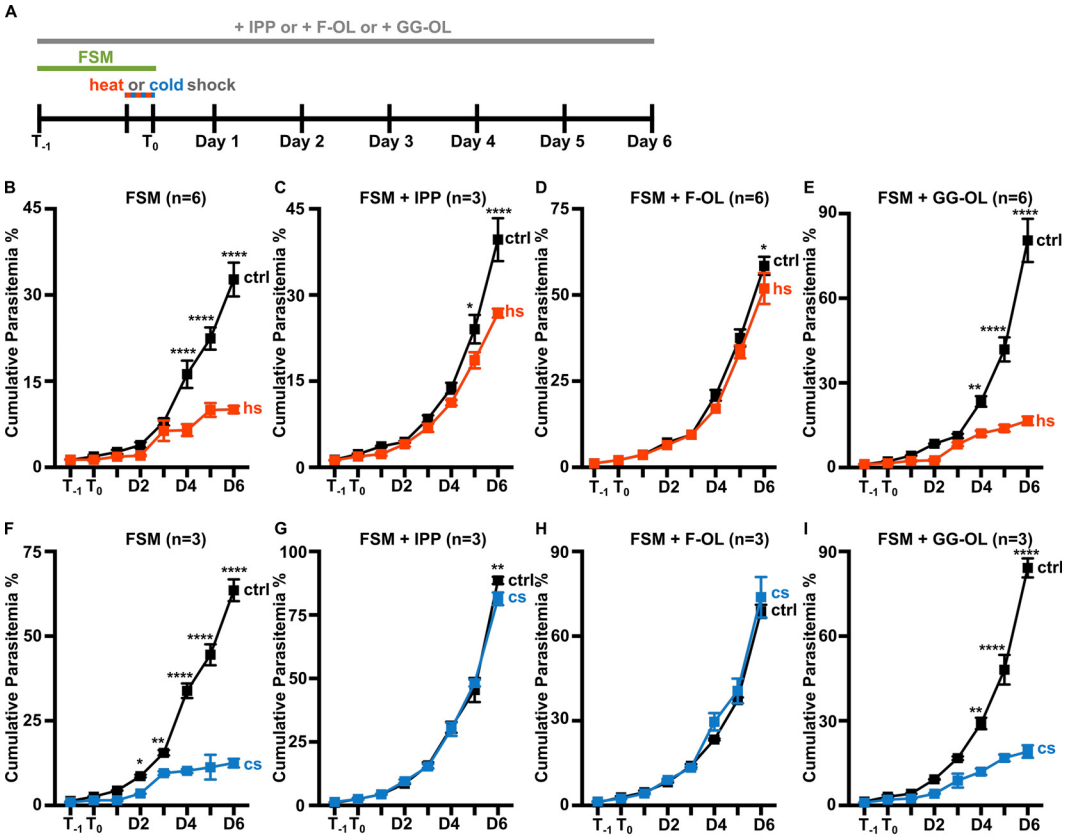

FIG 2 Supplementation with IPP and F-OL rescues growth in FSM-treated parasites after temperature stress. (A) Parasites were treated with FSM (5 μM) for 24 h prior to a 6-h heat (40°C) or cold (25°C) shock. Cultures were supplemented with isoprenoid products (IPP [250 μM], F-OL [10 μM], or GG-OL [10 μM]) for the entire length of experiment. (B) FSM-treated parasites are sensitive to heat shock. (C and D) Supplementation with IPP (C) or F-OL (D) rescues heat sensitivity. (E) GG-OL supplementation is unable to rescue growth after heat stress. (F to I) IPP or F-OL, but not GG-OL, supplementation is similarly able to rescue FSM-treated parasite growth after cold shock. (B to I) n = 3 to 6; *, $P \leq 0.05$; **, $P \leq 0.01$; ***, $P \leq 0.001$; ****, $P \leq 0.0001$. Two-way ANOVA, P values adjusted for multiple comparisons using Sidak's multiple-comparison test. Abbreviations: ctrl, control, hs, heat shock, cs, cold shock.

asexual blood-stage growth (45). To address the role of HSP40 in asexual development, we sought to disrupt the HSP40 locus directly. Using single-crossover homologous recombination (as previously used to validate the MEP pathway genes, Dxr and IspD) (20, 46), we successfully integrated a control plasmid into the HSP40 genetic locus (Fig. S3A and B). However, even after 7 months of continuous culture, integration of a disruption construct did not occur (Fig. S3A). Our data support an essential role for HSP40 in the parasite during blood-stage growth.

HSP40 can stimulate ATPase activity of its cochaperone HSP70 *in vitro*. In contrast to the highly expanded HSP40 protein family, the *P. falciparum* genome encodes only 6 Hsp70-like proteins (34, 47). HSP70 (PF3D7_0818900), the major cytosolic Hsp70 in *P. falciparum*, possesses ATPase activity and is itself important for thermal tolerance in the parasite (32, 48–50). Select Hsp40 cochaperones interact with Hsp70 through a protein domain called a J domain (51–55). To determine whether HSP40 interacts with HSP70 to promote ATP hydrolysis, recombinant 6×His-HSP40 and 6×His-HSP70 were expressed and purified from *Escherichia coli* (Fig. S4A). We found that the addition of purified recombinant HSP40 stimulates the basal ATP hydrolytic activity of HSP70 (Fig. S4B and C). Increasing the amount of HSP70 in the reaction increases ATP turnover (Fig. S4D); however, the addition of HSP40 increases the ATPase activity of HSP70 nearly 3-fold (Fig. S4C). These data, along with previous observations by Botha et al. (36), confirm the functional interaction between HSP40 and HSP70.

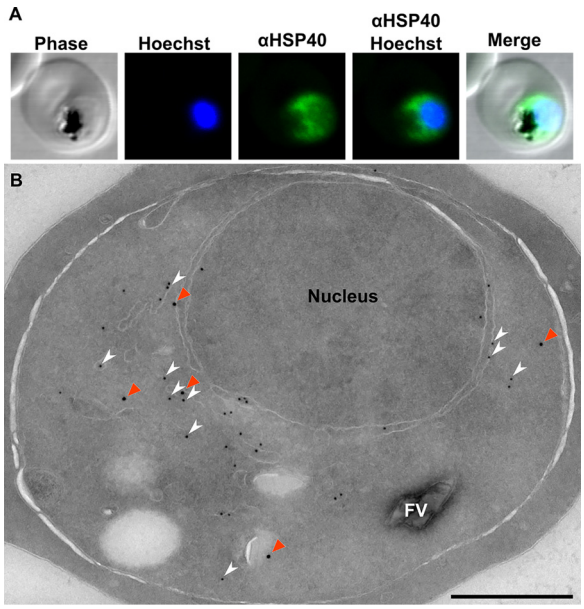

FIG 3 Localization of HSP40 in *P. falciparum*. (A) Immunofluorescence confocal microscopy of trophozoite, stained with anti-HSP40 (1:5,000) and Hoechst 33258 nuclear stain. HSP40 appears cytosolic. (B) Electron micrograph of immunolabeling: primary, rabbit anti-HSP40 (1:250), mouse anti-PDI (1:100); secondary, goat anti-rabbit IgG 18 nm colloidal gold, goat anti-mouse 12 nm. HSP40 (orange arrowheads) looks cytosolic in the parasites, with some apparent membrane association. A portion of HSP40 colocalizes with PDI, an established ER marker (white arrowheads). Scale, 500 nm.

Robust HSP40 membrane association requires IPP synthesis and protein farnesylation. Using purified recombinant 6×His-HSP40 (Fig. S4A), polyclonal antisera were generated. Immunoblotting with anti-HSP40 antisera revealed a single band in parasite lysate, which is not present in uninfected red blood cells (RBCs) (Fig. S4E and F). Antisera specificity was confirmed by immunoprecipitation (IP) and mass spectrometry, demonstrating exclusive immunoprecipitation of HSP40 without cross-reactivity to other Hsp40 family members in *P. falciparum* (Fig. S4G).

Since heat shock proteins help mediate export of parasite proteins through the PTEX complex (56–58), we performed immunofluorescence localization of HSP40 in asexual *P. falciparum*. HSP40 localizes to the parasite cytosol in trophozoite-stage parasites and is not detected in the host cell (Fig. 3A). Immuno-electron microscopy (immuno-EM) was performed to further characterize the subcellular localization of HSP40. We found that HSP40 is distributed throughout the cytosol and excluded from the nucleus and host cell cytoplasm (Fig. 3B). Because farnesylation marks small GTPases for localization to the cytosolic face of the endoplasmic reticulum (ER) (59, 60), we predicted that some portion of HSP40 may be ER localized. In addition to anti-HSP40, parasites were labeled with anti-protein disulfide isomerase (anti-PDI), an established ER marker (61, 62). A subset of HSP40 (48.7% of all labeling) is localized alongside PDI in the ER (Fig. 3B). These data indicate that HSP40 is both cytosolic and ER localized.

HSP40 is found in the membrane fraction (Fig. 4A and B), following detergent fractionation of parasite lysate. While overall levels of HSP40 protein remain unchanged with inhibition of IPP synthesis or farnesylation, the percentage of membrane-associated HSP40 is significantly reduced (Fig. 4C and D). Treatment with farnesylation inhibitors (such as FTI or BMS), but not the geranylgeranylation inhibitor GGTI, reduces membrane-associated HSP40 (Fig. S5). Subcellular localization of HSP40 is changed after treatment with FTI (Fig. 4E). Quantification of immuno-EM micrographs confirms a reduced membrane association of HSP40 in inhibitor-treated cells (Fig. 4F). Overall, these observations provide evidence that a subset of HSP40 is membrane associated and that this membrane association requires farnesylation.

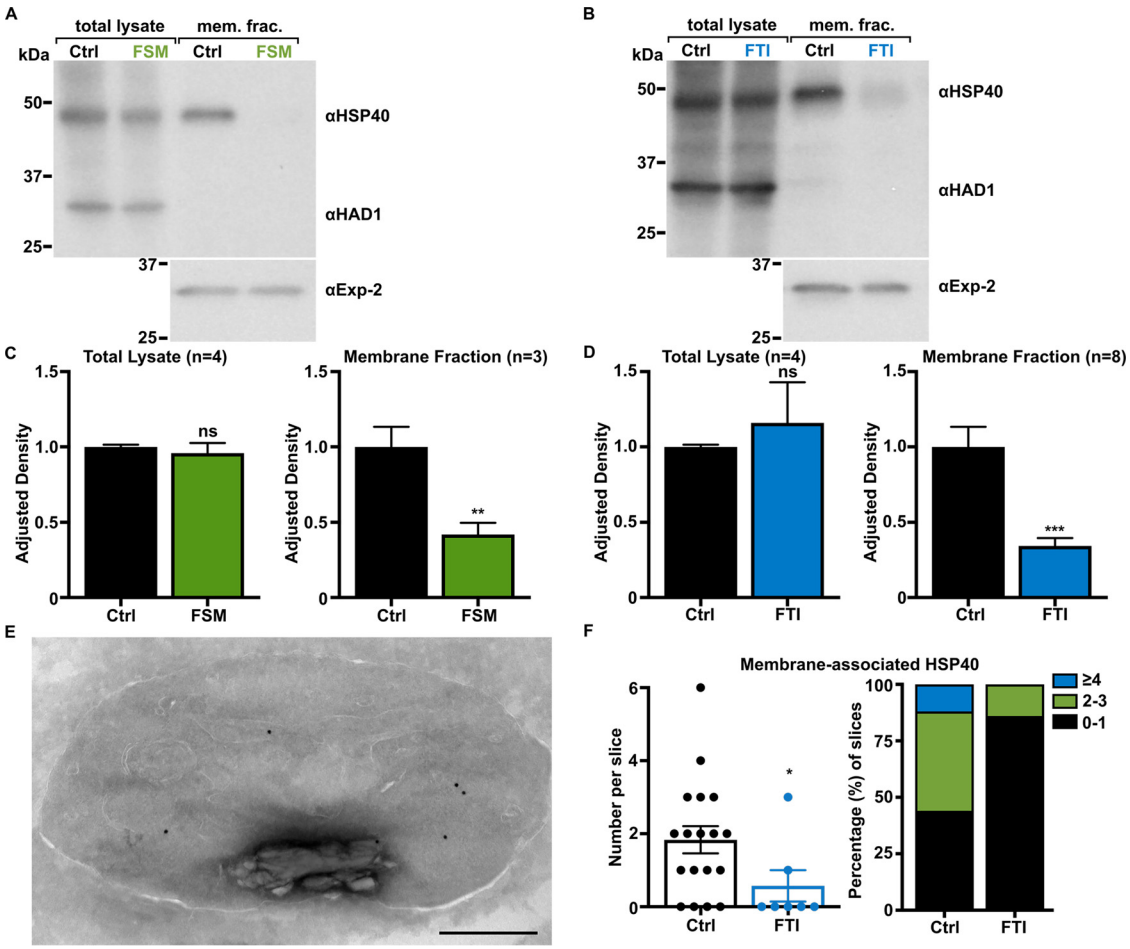

FIG 4 Inhibition of either IPP synthesis or protein farnesylation results in reduced membrane association of HSP40. (A and B) Representative anti-HSP40 immunoblots of control- and FSM (20 μM)-treated (A) or FTI (10 μM)-treated (B) *P. falciparum* total lysate and membrane fractions. (C and D) Quantification of several immunoblots adjusted to loading control. HSP40 is significantly reduced in the membrane fraction after inhibition of IPP synthesis (C) and inhibition of farnesylation (D). Anti-HAD1 and anti-Exp-2, loading controls for total lysate and membrane fractions, respectively. **, $P \leq 0.01$; ***, $P \leq 0.001$ unpaired *t* test with Welch's correction. (E and F) HSP40 membrane association is reduced after FTI treatment. Apparent membrane-associated HSP40 (10 nm gold particles) is reduced after inhibition of farnesylation. The number of membrane-associated HSP40 per micrograph is quantified for control and treated parasites (F). A single control cohort was quantified. A decrease in the number of membrane-associated HSP40 particles is observed. *, $P \leq 0.05$, unpaired *t* test with Welch's correction. Scale, 500 nm.

Palmitoylation contributes to HSP40 membrane association but not thermotolerance. Farnesylation is not the only posttranslational modification that is expected to bring HSP40 to the membrane, as HSP40 is also palmitoylated (63). To evaluate the role of palmitoylation in the membrane association of HSP40 and parasite thermotolerance, we employed the palmitoylation inhibitor, 2-bromopalmitate (2BP) (64). While overall levels of HSP40 remained unchanged upon inhibition of palmitoylation, the proportion of membrane-associated HSP40 was significantly reduced (Fig. 5A and B). Combined treatment with 2BP and FTI (to inhibit both palmitoylation and farnesylation) further reduced the levels of membrane-associated HSP40 compared to either treatment alone (Fig. 5A and B). We tested whether inhibition of palmitoylation influenced parasite growth following heat (40°C) or cold (25°C) stress. Consistent with our previous observations, untreated parasites readily recovered after modest heat or cold shock (Fig. 5C and G), while inhibition of farnesylation significantly impaired recovery after temperature stress (Fig. 5D and H). In contrast, treatment with 2BP did not sensitize parasites to temperature stress, as growth was unchanged following heat and cold shock (Fig. 5E and I). Loss of protein palmitoylation was also not protective, as parasites treated with both FTI and 2BP remained sensitive to temperature shock (Fig. 5F and J).

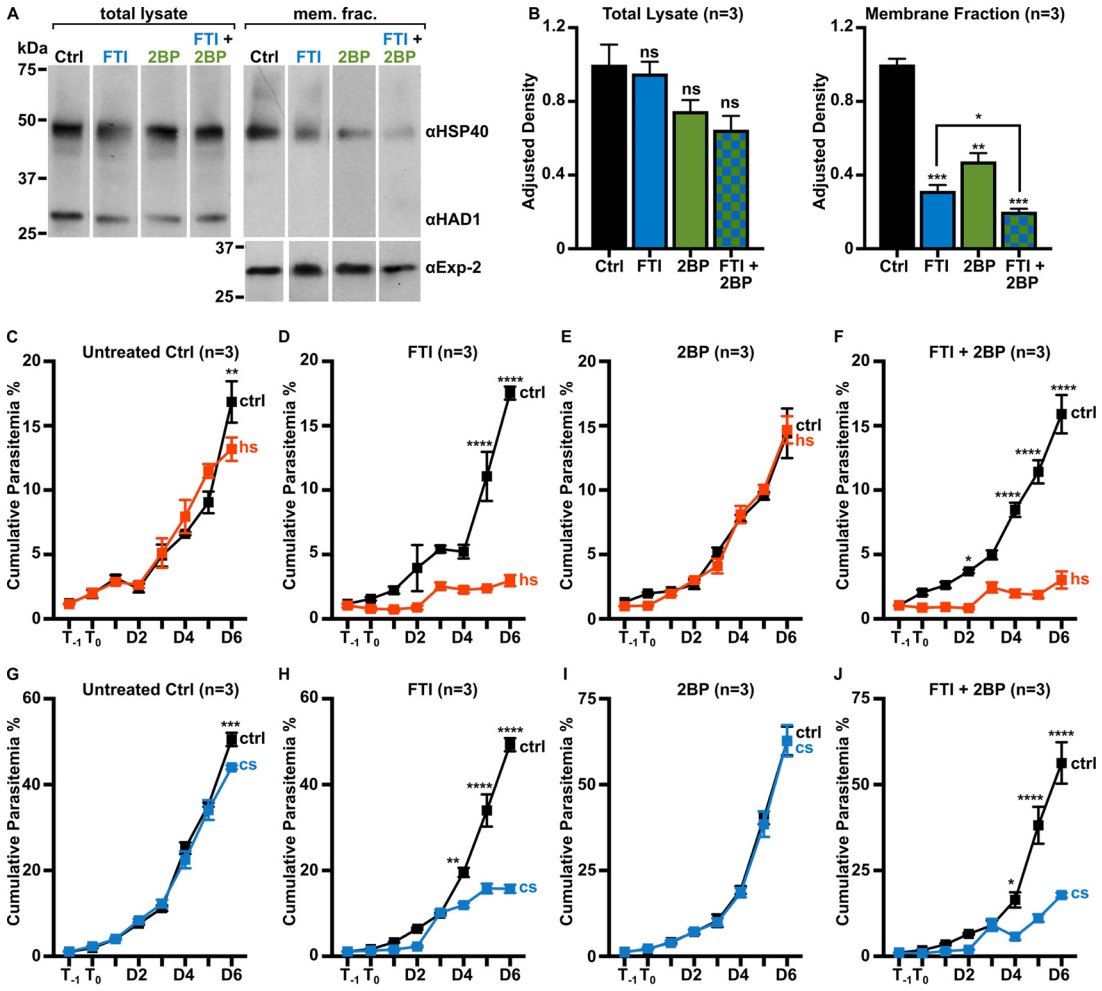

FIG 5 Both farnesylation and palmitoylation contribute to HSP40 membrane association, but only farnesylation is required for thermotolerance. (A) Representative anti-HSP40 immunoblots of control, FTI (10 μM), 2BP (100 μM), and combination of FTI- and 2BP-treated *P. falciparum* total lysate and membrane fractions. (B) Quantification of several immunoblots adjusted with loading control. The membrane-associated proportion of HSP40 is significantly reduced upon inhibition of farnesylation (FTI) or palmitoylation (2BP). Inhibition of both farnesylation and palmitoylation (FTI + 2BP) reduces HSP40 membrane association further than does single inhibitor treatment. Anti-HAD1 and anti-Exp-2, loading controls for total lysate and membrane fractions, respectively. $n = 3$; *, $P \leq 0.05$; **, $P \leq 0.01$; ***, $P \leq 0.001$ unpaired *t* test with Welch's correction. (C to J) Parasites were treated with FTI (10 μM), 2BP (100 μM), or both prior to heat (40°C) or cold (25°C) shock. FTI-treated parasite growth is significantly reduced after heat (D) and cold shock (H). Growth in 2BP-treated parasites is unchanged after heat or cold shock (E and I). Parasites treated with both FTI and 2BP were sensitive to temperature stress (F and J). $n = 3$; *, $P \leq 0.05$; **, $P \leq 0.01$; ***, $P \leq 0.001$; ****, $P \leq 0.0001$, 2-way ANOVA, *P* values adjusted for multiple comparisons using Sidak's multiple-comparison test. Abbreviations: ctrl, control; hs, heat shock; cs, cold shock.

Therefore, while palmitoylation helped facilitate membrane association of HSP40, farnesylation, not palmitoylation, was required for parasite stress survival.

Chemical inhibition of protein farnesylation alters the HSP40 interactome. HSP40 is expected to interact with numerous cochaperones and client proteins. Protein prenylation is known to drive association with the ER and is likely to alter accessibility to client proteins (65). Therefore, we determined whether loss of prenylation alters the array of cellular client proteins that bind to HSP40. We used immunoprecipitation and mass spectrometry to identify HSP40-interacting proteins from parasites under normal prenylation conditions (wild-type controls) and when prenylation was chemically impaired either through inhibition of isoprenoid biosynthesis (with FSM) or through inhibition of farnesyl transferase activity (with FTI).

We found that HSP40-interacting proteins mediated a number of essential biological functions in the parasite, including cytoskeleton organization, glycolysis, and translation

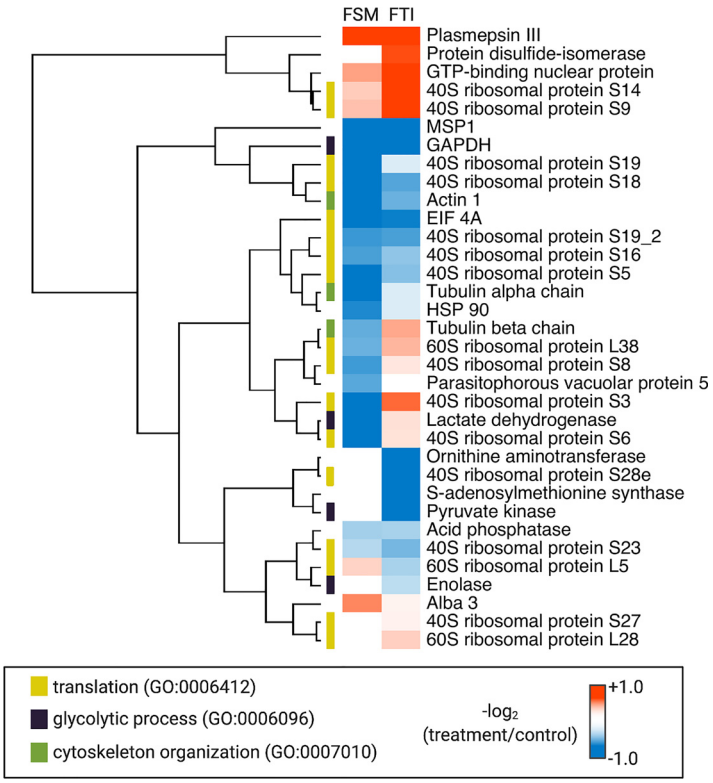

FIG 6 Both IPP synthesis and protein farnesylation influence HSP40 protein-protein interactions. Candidate protein interactors were determined by mass spectrometry after IP of parasite lysate with anti-HSP40. Results for FSM (5 μM)- and FTI (10 μM)-treated parasites are compared to untreated controls ($n = 3$). UniProt and GeneIDs are provided in Table S2. Heat map of normalized $\log_2$-transformed data was generated using NG-CHM Heat Map Builder. Gene Ontology (GO) annotations are indicated by colored bars.

(Table S1; Fig. 6; Table S2). When prenylation was reduced, either by reducing production of isoprenyl groups (with the isoprenoid biosynthesis inhibitor FSM) or by reducing transfer of prenyl groups (with the farnesyl transferase inhibitor FTI), the overall profile of client protein interactions was markedly altered. When prenylation is reduced, HSP40 had a reduced association with membranes and with the ER (Fig. 4). Loss of prenylation reduces association with a number of ribosomal proteins, consistent with reduced association with the rough ER. In addition, the interaction of HSP40 with the glycolytic enzyme GAPDH (glyceraldehyde-3-phosphate dehydrogenase) was reduced after treatment with either FSM or FTI (Fig. 6).

HSP40 farnesylation influences GAPDH localization but not its glycolytic function. The farnesylation-dependent interaction between HSP40 and GAPDH (PF3D7_1462800) drew special attention because GAPDH is essential for the glycolytic breakdown of glucose to produce ATP in the parasite. Isoprenoid biosynthesis is immediately metabolically downstream of glycolysis, and therefore we further investigated the role of prenylation in mediating membrane association and function of GAPDH. Using purified recombinant 6×His-GAPDH, specific polyclonal antisera were generated (Fig. S6A and B). As observed for HSP40, we found that GAPDH was, in part, membrane associated, as has been previously observed (66, 67). We found that this association was dependent on both IPP synthesis and farnesylation (Fig. 7A to C).

To understand whether interrupting IPP synthesis and protein prenylation directly affects glycolytic function in the parasite, we quantified glycolytic intermediates in the presence and absence of IPP synthesis and protein prenylation. We found that the cellular levels of the products of glycolysis including pyruvate and lactate were unchanged after treatment with either FSM or FTI (Fig. 8). Substrate availability to the pentose phosphate pathway also did not change upon FSM or FTI treatment (Fig. 8). Our data indicate that,

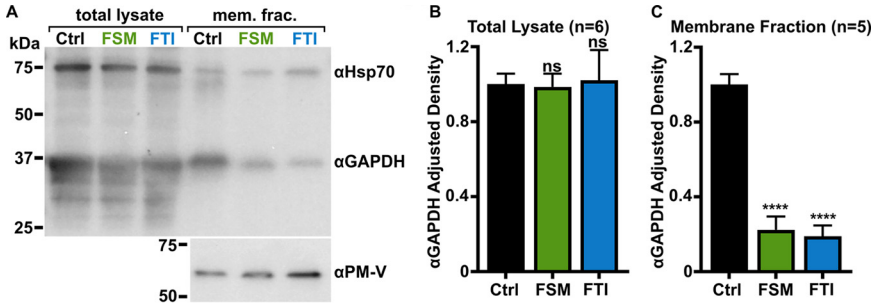

FIG 7 Localization of GAPDH, but not its glycolytic function, is IPP- or farnesylation-dependent. (A to C) Inhibition of IPP synthesis and farnesylation reduced membrane association of GAPDH. (A) Representative anti-GAPDH immunoblots of control-, FSM (20 μM)-, and FTI (10 μM)-treated *P. falciparum*. (B and C) Quantification of several immunoblots adjusted with loading control. Anti-Hsp70 (1:5,000) and anti-PM-V (1:500) were used as loading controls for total lysate and membrane fractions, respectively. $n = 5$ to 6; ****, $P \leq 0.0001$, unpaired t test with Welch's correction.

although the interaction between HSP40 and glycolytic enzymes is prenylation-dependent, farnesylation does not directly influence glycolytic function in the parasite.

DISCUSSION

Temperature change is a critical environmental signal and an integral environmental stress of the *P. falciparum* life cycle. In addition, antimalarial activity of the first-line artemisinin-based therapies may be sensitive to heat or cold stress (6, 8). However, the mechanisms by which the parasite copes with thermal stress are not well understood, and the inherent host temperature fluctuations during clinical malaria may be exploited to improve malaria treatment. In this study, we reveal that survival during heat or cold shock in *P. falciparum* requires both *de novo* isoprenoid biosynthesis and the posttranslational 15-carbon isoprenyl modification called farnesylation. Chemical inhibitors that reduce protein farnesylation, by reducing either isoprenoid biosynthesis or farnesyltransferase activity, sensitize *P. falciparum* to otherwise nonlethal temperature stresses, even at otherwise subinhibitory doses. Our observations are supported by a parallel study by Zhang et al. (68), which also identified isoprenoid biosynthesis as critical for survival of *P. falciparum* at febrile temperatures, using a large-scale piggyBac transposon mutant phenotypic screen. Together, these observations suggest that isoprenoid and prenylation inhibitors might be particularly valuable in the setting of malarial fever, a nearly universal characteristic of symptomatic *P. falciparum* infection (69).

Housed within the apicoplast organelle, isoprenoid biosynthesis through the MEP pathway is necessary for intraerythrocytic development of *P. falciparum* (18–20). Isoprenyl modification of proteins is a key essential function of the MEP pathway, as prenylation itself is essential for asexual development (23–27). However, the pleiotropic downstream effects brought on by loss of protein prenylation have not been fully elucidated. Kennedy et al. recently proposed a mechanistic model of "delayed death," a phenotype of parasite demise during the second erythrocytic cycle following drug treatment, exhibited by antimalarials that target apicoplast maintenance. In this model, disruption of Rab protein geranylgeranylation and interruption of subsequent cellular trafficking are responsible for the growth arrest caused by loss of IPP production or protein prenylation (70). Geranylgeranylated Rab GTPase family members comprise the majority of prenylated proteins in *P. falciparum* (30, 31). Rab GTPases are also believed to contribute to the structural integrity of the digestive food vacuole of the parasite (23), which is linked to thermal tolerance (32). However, our data suggest that the phenotype in malaria parasites caused by loss of isoprenoid biosynthesis or protein prenylation is more complicated and that interruption of protein farnesylation (even when geranylgeranylation is preserved) also plays an important role. Both geranylgeranylation of Rab GTPases and farnesylation, likely of HSP40, are key to the essential nature of prenylation in *P. falciparum*.

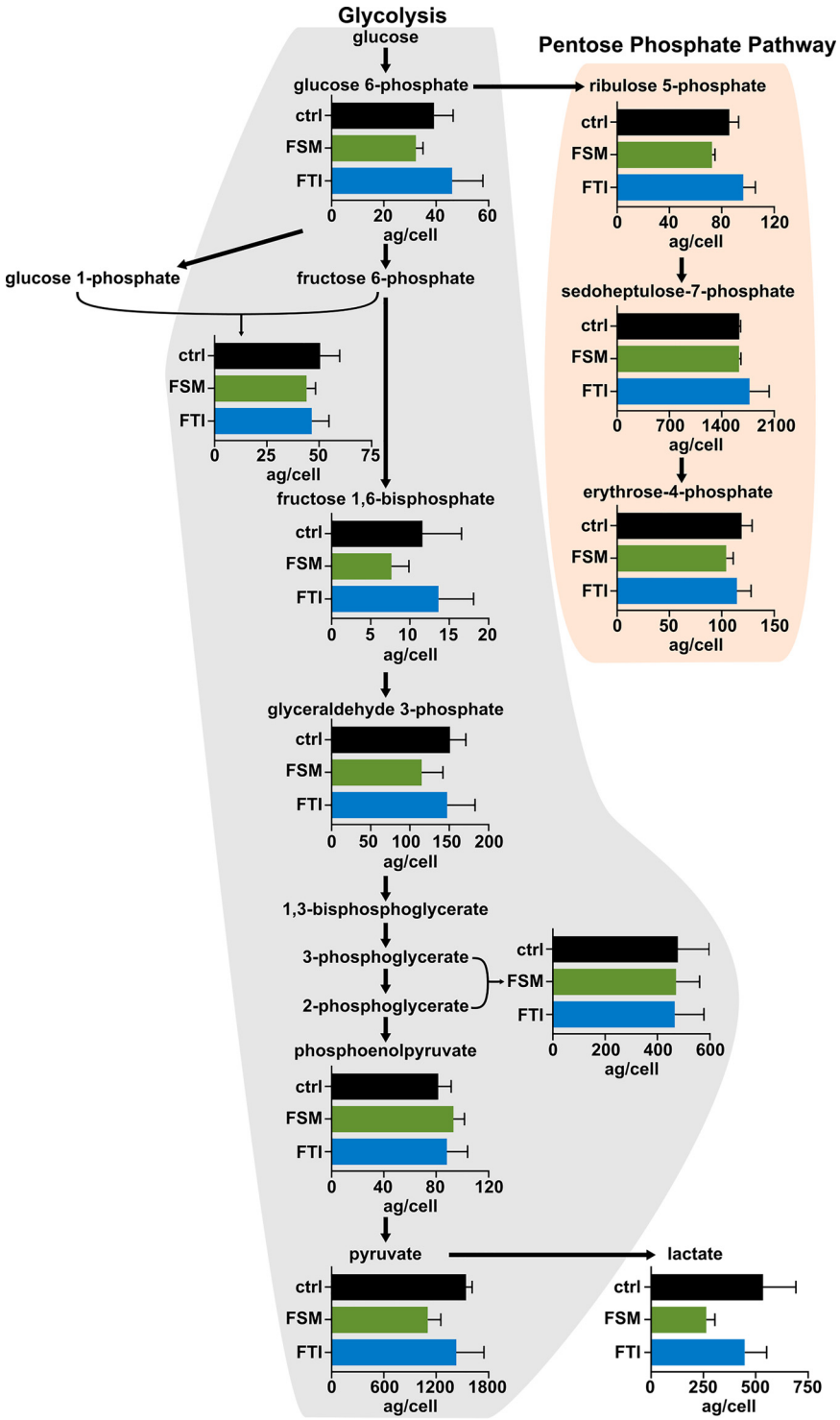

FIG 8 Glycolytic and pentose phosphate pathway metabolite levels remain constant under IPP- and farnesylation-deficient conditions. Levels of glycolytic and pentose phosphate pathway intermediates were measured by liquid chromatography with tandem mass spectrometry and normalized based on parasitemia of each individual sample to give concentration per cell. No significant changes are observed after treatment with FSM (5 μM) or FTI (10 μM). $n = 3$, unpaired t test with Welch's correction.

Our data also suggest the presence of several distinct cellular pools of HSP40 that have different posttranslational modifications, subcellular localizations, and client protein interactomes. Maximal membrane association of HSP40 requires posttranslational palmitoylation. Palmitoylation may guide HSP40 to a membrane subcompartment that

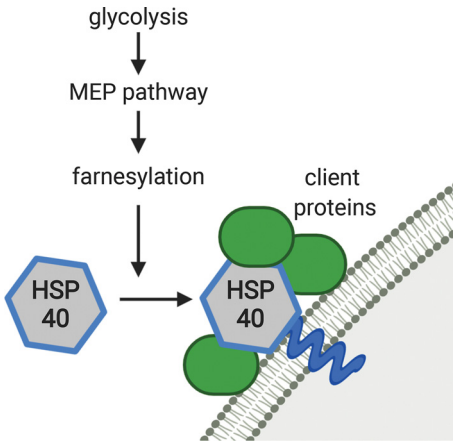

FIG 9 Isoprenoid biosynthesis and farnesylation affect membrane association and client protein assembly of HSP40.

is different from that of farnesyl-HSP40. Similar findings have been described for mammalian Ras proteins, which, as for HSP40, are both farnesylated and palmitoylated. For Ras proteins, both posttranslational modifications are needed for stable plasma membrane association (71). As palmitoylation is not required for parasite thermotolerance, palmitoyl-HSP40 appears to have other, yet-unidentified functions in malaria parasites.

While heat shock proteins are found across taxa, not all organisms possess prenylated Hsp40s (72). HSP40 orthologs in human, yeast, *Plasmodium* spp. (*P. vivax*, *P. yoelii*, *P. chabaudi*, and *P. berghei*), and plants (*Arabidopsis thaliana* and *Atriplex nummularia*) have been experimentally demonstrated to be prenylated or are predicted to be prenylated based on the presence of canonical C-terminal prenylation sequence motifs (37, 73–75). It is unclear how the function of Hsp40 orthologs might differ in organisms that lack prenylated Hsp40s. However, our data, in conjunction with studies in yeast and plants, provide compelling evidence that prenylation of Hsp40 has evolved for survival during environmental stress, including growth after temperature or drought stress (37–39, 74, 76, 77). HSP40 is one of only 4 farnesylated proteins in *P. falciparum* and the sole farnesylated heat shock protein (30, 31). We find that farnesylation controls membrane association of HSP40 on the endoplasmic reticulum, modulates access to its client proteins, and is necessary for survival during temperature stress (Fig. 9). Together, these observations suggest that prenylation of Hsp40 is a marker that distinguishes a distinct functional subclass of Hsp40s which appear to play similar cellular roles in animals, plants, and fungi and have essential functions in environmental stress responses that are conserved across the domains of life.

Our data suggest that compounds that target IPP synthesis or farnesylation may be more effective *in vivo* than *in vitro*, as parasites cycle through host temperature changes. As Hsp40 cochaperone family members are amenable to small molecule inhibition (78, 79), a combination therapy that targets both protein prenylation and heat shock proteins directly has the potential to be highly parasiticidal. In addition, Hsp40 function is likely important to survival under artemisinin treatment. Whole-genome sequencing of clinical parasite samples collected during the emergence of artemisinin resistance in Thailand revealed a nonsynonymous mutation in Hsp40 that may provide a suitable background for artemisinin resistance mutations (80). A recent study indicates that the *P. falciparum* transcriptional response to heat stress and artemisinin are highly correlated (68). Targeting apicoplast function, prenylation, or heat shock also hold promise as adjunctive therapies to reverse artemisinin susceptibility.

MATERIALS AND METHODS

Materials. All buffer components, salts, and enzyme substrates were purchased from Millipore Sigma (Burlington, MA), unless otherwise indicated.

Statistical analysis. We plotted all data and performed all statistical analyses in GraphPad Prism software (version 8). All data are expressed as the mean ± standard error of the mean (SEM). For

statistical analysis, we used 2-way analysis of variance (ANOVA), *t* test with Welch's correction, and multiple unpaired *t* test to compare results. To understand the interaction between treatment and temperature stress, we utilized a 2-way ANOVA and then adjusted *P* values for multiple comparisons using Sidak's multiple-comparison test. For direct comparisons between control and treatment groups, we employed *t* test with Welch's correction because standard deviations were not the same between groups. Mass spectrometry data were analyzed using multiple *t* tests to efficiently compare results across conditions for each protein.

Drug inhibitors and isoprenoids. Fosmidomycin (50 mM; Millipore Sigma), FTI-277 (5 mM; Tocris Bioscience, Bristol, UK), and IPP (30 mM; Echelon Biosciences, Salt Lake City, UT) were each dissolved in water at concentrations indicated. GGTI-298 (20 mM; Cayman Chemical, Ann Arbor, MI), BMS-388891 (20 mM; kindly provided by Wesley Van Voorhis, University of Washington), 2-bromopalmitate (100 mM; Millipore Sigma), farnesol (50 mM; Millipore Sigma), and geranylgeraniol (50 mM; Echelon Biosciences) were each dissolved in 100% dimethyl sulfoxide (DMSO) at concentrations indicated.

Parasite strains and culture. Unless otherwise indicated, parasites were maintained at 37°C in 5% O_2–5% CO_2–90% N_2 in a 2% suspension of human erythrocytes in RPMI medium modified with 27 mM $NaHCO_3$, 11 mM glucose, 5 mM HEPES, 0.01 mM thymidine, 1 mM sodium pyruvate, 0.37 mM hypoxanthine, 10 μg/ml gentamicin, and 5 g/liter Albumax (Thermo Fisher Scientific, Waltham, MA). All experiments were conducted in wild-type strain 3D7 (MRA-102) obtained through the MR4 as part of the BEI Resources Repository, NIAID, NIH.

Heat and cold shock *P. falciparum* growth assays. Asynchronous cultures were diluted to 1% parasitemia. Cultures were treated with indicated drugs 24 h prior to a 6-h heat shock (40°C) or cold shock (25°C). Media (no drug) were exchanged post temperature shock. Cultures were split 1:6 after the collection of the day 2 sample. IPP, F-OL, and GG-OL were supplemented in fresh media every second day. Samples were taken at indicated time points and fixed in phosphate-buffered saline (PBS)–4% paraformaldehyde. Cells were stained with 0.01 mg/ml acridine orange, and parasitemia was determined on a BD Biosciences LSRII flow cytometer (Thermo Fisher Scientific). All data represent means of results from ≥3 independent experiments using biological replicates.

pCAM-BSD HSP40 plasmid construction. Functional genetic validation of HSP40 (PF3D7_1437900) was performed as described previously for PfDXR (20) and PfIspD (46). pCAM-BSD-HSP40^{KO} and pCAM-BSD-HSP40^{ctrl} vectors were derived from pCAM-BSD (gift from David Fidock, Columbia University), which includes a blasticidin-resistance cassette under transcriptional control by the *P. falciparum* D10 calmodulin 5′ untranslated region (UTR) and the 3′ UTR of HRP2 from *P. berghei*. To construct pCAM-BSD-HSP40^{KO}, the coding sequence for a segment of HSP40 near the N terminus (bp 29 to 878) was inserted directly into 5′ of the *P. berghei* dihydrofolate reductase (DHFR)-thymidylate synthase 3′ UTR. This insert was constructed by PCR using primers (A) 5′-CCCGGGACTCTATGGGTGGTCAACAAG-3′ and (B) 5′-CTCGAGTCTCATGTAGGTCTTGGTTCC-3′ and restriction cloned using *Xma*I and *Xho*I sites. pCAM-BSD-HSP40^{ctrl} contained the coding sequence for the C-terminal end of HSP40 (bp 963 to 1619) and 237 bp of the 3′ UTR, generated using (C) 5′-CCCGGGGAGGAACCAAGACCTACATGAG-3′ and (D) 5′-CTCGAGCATTTCACAGACACACACACAC-3′ as primers. This sequence was inserted at the same site, 5′ of the *P. berghei* DHFR-thymidylate synthase 3′ UTR. All constructs were verified by Sanger sequencing.

Parasite transfections. Transfections were performed as described previously (46). Briefly, 150 μg of plasmid DNA was precipitated and resuspended in Cytomix (25 mM HEPES [pH 7.6], 120 mM KCl, 0.15 mM $CaCl_2$, 2 mM EGTA, 5 mM $MgCl_2$, 10 mM K_2HPO_4). A ring-stage *P. falciparum* culture was washed with Cytomix and resuspended in the DNA/Cytomix solution. Cells were electroporated using a Bio-Rad Gene Pulser II electroporator at 950 μF and 0.31 kV. Electroporated cells were washed with media and returned to normal culture conditions. Parasites expressing the construct were selected by continuous treatment with 2 μg/ml blasticidin S HCl (Thermo Fisher Scientific). Transfectants were cloned by limiting dilution, and diagnostic PCRs were performed using genomic DNA from resultant transfectants using primer sets specific for episomal plasmids or genome integrants. Primer A and D sequences are as follows: (X) 5′-TAAGAACATATTTATTAAACTGCAG-3′; (Y) 5′-GAAAAACGAACATTAAGCTGCCATA-3′.

Southern blotting. Southern blotting was used to assay the integration of the pCAM-BSD-HSP40^{ctrl} plasmid. To assay the integration of pCAM-BSD-PfHsp40^{ctrl}, genomic DNA was harvested from wild-type 3D7 *P. falciparum* and from the continuously cultured pCAM-BSD-HSP40^{ctrl} transfectants 1, 2, 3, and 4 from Fig. S3. These genomic DNA samples, along with pCAM-BSD-HSP40^{ctrl} plasmid, were digested with SmlI (New England Biolabs). The control probe was prepared from PCR product generated using primers (HSP40_Ctrl_F) 5′-GAGGAACCAAGACCTACATGAG-3′ and (HSP40_Ctrl_R) 5′-ATGATCTTCATCGTCGTATGC-3′ (HSP40 bp 856 to 1,574) prior to Southern blotting.

Generation of recombinant HSP40, HSP70, and GAPDH. An *E. coli* codon optimized HSP40 was produced (Genewiz, South Plainfield, NJ) and inserted via ligation-independent cloning into the isopropyl-β-D-1-thiogalactopyranoside (IPTG) inducible BG1861 expression vector. This created an N-terminal 6×His tag fusion protein used for nickel purification. The expression plasmid was transformed into One Shot BL21(DE3)pLysS *E. coli* cells (Thermo Fisher Scientific). Overnight, starter cultures were diluted 1:1,000 and grown to an optical density (OD) of ~0.6 where 1 mM IPTG was added for 16 h at 16°C. Cells were spun and stored at −80°C. Recombinant HSP70 (PF3D7_0818900) was expressed using the same conditions. In a similar manner, an *E. coli* codon optimized GAPDH (PF3D7_1462800) was produced with a few minor experimental differences. The GAPDH expression plasmid was transformed into One Shot BL21(DE3) *E. coli* cells (Thermo Fisher Scientific). One mM IPTG was added for 2 h at 37°C.

Expressed proteins were purified from cells using a sonication lysis buffer containing 1 mg/ml lysozyme, 20 mM imidazole, 1 mM dithiothreitol, 1 mM $MgCl_2$, 10 mM Tris-HCl (pH 7.5), 30 U benzonase, 1 mM phenylmethylsulfonyl fluoride (PMSF), and cOmplete EDTA-free protease inhibitor tablets (Roche, Basel,

Switzerland). Lysates were clarified using centrifugation, and proteins were purified via nickel agarose beads (Gold Biotechnology, Olivette, MO), eluted with 300 mM imidazole, 20 mM Tris-HCl (pH 7.5), and 150 mM NaCl. Eluted proteins were further purified via size exclusion chromatography using a HiLoad 16/60 Superdex 200 gel filtration column (GE Healthcare, Chicago, IL) using an AKTAExplorer 100 fast protein liquid chromatography (FPLC) system (GE Healthcare). Fast protein liquid chromatography buffer contained 100 mM Tris-HCl (pH 7.5), 1 mM $MgCl_2$, 1 mM dithiothreitol (DTT), and 10% wt/vol glycerol. HSP70 and GAPDH fractions containing purified protein were individually pooled, concentrated to ~2 mg/ml as determined via Pierce BCA protein assay kit (Thermo Fisher Scientific), and stored by adding 50% glycerol for storage at −20°C. HSP40 fractions containing purified protein were pooled and further purified via anion exchange using a Mono Q anion exchange chromatography column (GE Healthcare) using an AKTAExplorer 100 FPLC (GE Healthcare). Anion exchange buffer contained 100 mM Tris-HCl (pH 8.0), 1 mM $MgCl_2$, and 100 mM NaCl. Purified fractions were concentrated to ~2 mg/ml as determined via Pierce BCA protein assay kit (Thermo Fisher Scientific), glycerol was added to reach a concentration of 10% (wt/vol), and protein solutions were immediately flash frozen and stored at −80°C.

HSP70 ATPase activity assays. Hydrolysis of ATP by HSP70 was measured using an EnzChek phosphate assay kit (Thermo Fisher Scientific). All reaction mixtures contained 50 mM ATP. HSP70 was added to the reaction ranging from 9 to 45 μg. HSP40 was used in reactions at 8.9 μg. Absorbance was measured every 12 s for 40 min. Slopes were calculated by using the nonlinear regression analysis tool in Prism (GraphPad Software). All data represent means of results from ≥3 independent experiments using biological replicates and performed with technical replicates.

HSP40 and GAPDH antiserum generation. HSP40 and GAPDH rabbit polyclonal antisera was generated by Cocalico Biologicals (Reamstown, PA) using their standard protocol. Purified 6×His-HSP40 or 6×His-GAPDH was used as the antigen and TiterMax was used as an adjuvant. Antiserum specificity was confirmed by immunoblotting of parasite lysate, RBCs, and purified protein. Further confirmation of anti-HSP40 specificity was conducted by performing immunoprecipitation (IP) analysis (discussed in "Immunofluorescence and immuno-EM," below).

Immunofluorescence and immuno-EM. For immunofluorescence labeling, infected RBCs at ~8% parasitemia were fixed with 4% paraformaldehyde diluted in PBS. Cultures were treated with indicated drugs 24 h prior to collection. Fixed cells were washed with 50 mM ammonium chloride, permeabilized by treatment with 0.075% NP-40 in PBS, and blocked using 2% bovine serum albumin in PBS. Cells were incubated with 1:5,000 rabbit polyclonal anti-HSP40 (described in "HSP40 and GAPDH antiserum generation," above). Hoechst 33258 (Thermo Fisher Scientific) was used as a nuclear counterstain. Dilutions of 1:1,000 of Alexa Fluor 488 goat anti-rabbit IgG (Thermo Fisher Scientific, A11008) were used as a secondary antibody. Images were obtained on an Olympus Fluoview FV1000 confocal microscope. For all immunofluorescence, minimal adjustments in brightness and contrast were applied equally to all images.

For immuno-EM, parasites were cultured at 2% hematocrit until they reached ~6 to 8% parasitemia. Cultures were treated with indicated drugs 24 h prior to collection. Parasites were magnetically sorted from uninfected RBCs and ring-stage parasites via MACS LD separation columns (Miltenyi Biotech, Bergisch Gladbach, Germany). Parasites were collected by centrifugation and fixed for 1 h on ice in 4% paraformaldehyde in 100 mM PIPES [piperazine-*N*,*N*′-bis(2-ethanesulfonic acid)]/0.5 mM $MgCl_2$ (pH 7.2). Samples were then embedded in 10% gelatin and infiltrated overnight with 2.3 M sucrose/20% polyvinylpyrrolidone in PIPES/$MgCl_2$ at 4°C. Samples were frozen in liquid nitrogen and then sectioned with a Leica Ultracut UCT7 cryo-ultramicrotome (Leica Microsystems, Wetzlar, Germany). Fifty-nm sections were blocked with 5% fetal bovine serum/5% normal goat serum for 30 min and subsequently incubated with primary antibody for 1 h at room temperature. Primary antibodies used include anti-HSP40 (1:250) and anti-PDI (1D3) mouse 1:100 (ADI-SPA-891-D; Enzo Life Sciences, Farmingdale, NY). Secondary antibodies were added at 1:30 for 1 h at room temperature. Secondary antibodies included 12 nm Colloidal Gold AffiniPure goat anti-mouse IgG (H + L) (115-205-146; Jackson ImmunoResearch, West Grove, PA) and 18 nm Colloidal Gold AffiniPure goat anti-rabbit IgG (H + L) (111-215-144; Jackson ImmunoResearch). Sections were then stained with 0.3% uranyl acetate/2% methyl cellulose and viewed on a JEOL 1200 EX transmission electron microscope (JEOL USA Inc., Peabody, MA) equipped with an AMT 8 megapixel digital camera and AMT Image Capture Engine V602 software (Advanced Microscopy Techniques, Woburn, MA). All labeling experiments were conducted in parallel with controls omitting the primary antibody. Quantification of membrane-associated HSP40 was performed in micrographs where both a nucleus and food vacuole were present. Images were blinded and scored for total number labeled HSP40 and membrane-associated HSP40 (defined as being on or directly touching a well-visualized membrane).

Membrane fraction preparation and immunoblotting. Cultures were treated with indicated drugs 24 h prior to collection. Asynchronous parasites were released from RBCs with 0.1% saponin, washed in cold PBS, and resuspended in 100 to 300 μl deionized (DI) water with 1 mM PMSF and cOmplete EDTA-free protease inhibitor tablet (Roche). Resuspended pellets were freeze-thawed three times with liquid nitrogen/37°C water bath. A total lysate sample was taken at this point in the protocol. The membranes were pelleted (14,000 RPM, 30 min, 4°C), and the supernatant was collected as the soluble fraction. Pellets were washed once with ice-cold PBS and pelleted (as before) before pellets were resuspended in 100 to 300 μl (depending on sample amount) radioimmune precipitation assay (RIPA) buffer (Cell Signaling Technology, Danvers, MA) containing 1% CHAPS {3-[(3-cholamidopropyl)-dimethylammonio]-1-propanesulfonate} and 1% ASB-14 (amidosulfobetaine-14). Samples were sonicated three times with a microtip and incubated at 42°C with shaking at 800 RPM for 45 min. The samples were then centrifuged (14,000 RPM, 30 min, 4°C), and the resulting supernatant was collected as the membrane fraction. A sample buffer of 4× SDS was added, and samples were boiled for 10 min and loaded on 4 to 20% mini-PROTEAN TGX gradient gels (Bio-Rad Laboratories, Hercules, CA).

For immunoblotting, proteins were transferred onto PVDF using wet transfer with 20% methanol. Blots were blocked either 1 h at 25°C or overnight at 4°C with 2% bovine serum albumin–0.1% Tween 20–PBS. Primary antibodies were used at the following dilutions: 1:5,000 rabbit anti-HSP40, 1:5,000 rabbit anti-GAPDH, 1:10,000 rabbit anti-HAD1 (81), 1:5,000 rabbit anti-Hsp70 (AS08 371; Agrisera Antibodies, Vännäs, Sweden), 1:500 mouse anti-PM-V (82), and 1:5,000 mouse anti-EXP-2 clone 7.7 (83). For all blots, 1:20,000 horseradish peroxidase (HRP)-conjugated goat anti-rabbit IgG antibody (Thermo Fisher Scientific, 65-6120) or 1:5,000 HRP-conjugated goat anti-mouse IgG antibody (Thermo Fisher Scientific, G-21040) was used as the secondary antibody. Anti-HAD1 or anti-Hsp70 and anti-PM-V or anti-Exp-2 were used as loading controls from total lysate and membrane fractions, respectively. All blot images are representative of results of a minimum of 3 independent experiments using biological replicates.

Immunoprecipitation of HSP40 from parasite lysate and protein mass spectrometry. Preinoculated rabbit antisera and anti-HSP40 were coupled to magnetic beads using the Dynabeads antibody coupling kit as per the manufacturer's protocol (Thermo Fisher Scientific, 14311D). Asynchronous parasite pellets (100 ml at 4% hematocrit and roughly 10% parasitemia) were harvested from RBCs using 0.1% saponin. Cultures were treated with indicated drugs 24 h prior to collection. Isolated parasite pellets were lysed in 300 μl of buffer containing 25 mM Tris-HCl (pH 7.5), 100 mM NaCl, 5 mM EDTA, 0.5% Triton-X 100, and 1 cOmplete mini EDTA-free protease inhibitor tablet (Roche) (per 10 mL of buffer). Resuspended pellets were homogenized using a LabGEN homogenizer (Cole-Parmer, Vernon Hills, IL) in 3 rounds of 30-s intervals with 60 s of rest on ice. Lysate was centrifuged at 14,000 RPM for 10 min at 4°C. The resulting soluble lysate was diluted by adding 450 μl of binding buffer containing 25 mM Tris-HCl (pH 7.5) and 150 mM NaCl. Diluted lysate was added to antisera-coupled beads that were previously washed three times with the same binding buffer. Lysate and beads were rotated for 2 h at 4°C. Beads were then washed three times with wash buffer (25 mM Tris-HCl [pH 7.5] and 500 mM NaCl) and flowthrough was discarded. Immunoprecipitated proteins were eluted using elution buffer with 200 mM glycine (pH 2.5) for 30 s, and eluted sample was neutralized with 1 M Tris-HCl (pH 7.5). Samples were then flash frozen and stored at −80° for immunoprecipitate identification via protein mass spectrometry.

Immunoprecipitates were identified via protein mass spectrometry by the Proteomics and Mass Spectrometry Core at the Donald Danforth Plant Science Center (St. Louis, MO) and analyzed by the Proteomics Core facility of the Children's Hospital of Philadelphia. Stored samples were submitted in solution for protein mass spectrometry. Protein and peptide identification/quantification was performed with MaxQuant (1.6.14.0) using a *Plasmodium falciparum* reference database from UniProt (UP000001450). Carbamidomethyl of Cys was defined as a fixed modification. Oxidation of Met and acetylation of protein N-terminal were set as variable modifications. Trypsin/P was selected as the digestion enzyme, and a maximum of 3 labeled amino acids and 2 missed cleavages per peptide were allowed. Fragment ion tolerance was set to 0.5 Da. The tandem mass spectrometry (MS/MS) tolerance was set at 20 ppm. The minimum peptide length was set at 7 amino acids. The false discovery rate for peptides and proteins was set at 1%. The rest of the parameters were kept as default.

Perseus (1.6.14.0) was used for proteomics data processing and statistical analysis. The MaxLFQ intensity values were used to analyze the whole-cell proteome data. Protein groups containing matches to decoy database or contaminants were discarded. The data were $\log_2$ transformed and normalized by subtracting the median for each sample. Proteins with fewer than two values in each group were filtered out. Nonspecific binding proteins were removed by filtering proteins that were enriched in pull-downs from prebleed sera. A heat map of normalized $\log_2$-transformed data was generated using NG-CHM Heat Map Builder (84). PANTHER 16.0 was used to annotate Gene Ontology (GO) terms for each gene (85, 86)

Metabolite profiling. A total of 60 ml of sorbitol-synchronized early trophozoites cultured at 4% hematocrit until it reached ~7 to 11% parasitemia was isolated using 0.1% saponin, washed with ice-cold PBS, and frozen at −80°C. Glycolysis and pentose phosphate pathway intermediates were extracted via the addition of glass beads (212 to 300 μm) and 600 μl chilled H_2O–chloroform–methanol (3:5:12 vol/vol) spiked with PIPES [piperazine-*N*,*N*′-bis(2-ethanesulfonic acid)] as the internal standard. The cells were disrupted with the TissueLyser II instrument (Qiagen, Hilden, Germany) using a microcentrifuge tubes adaptor set prechilled for 2 min at 20 Hz. The samples were then centrifuged at 16,000 × *g* at 4°C, the supernatants were collected, and the pellet extraction was repeated once more. The supernatants were pooled, and 300 μl of chloroform and 450 μl of chilled water were added to the supernatants. The tubes were vortexed and centrifuged. The upper layer was transferred to a new tube and dried using a speed-vac. The pellets were redissolved in 100 μl of 50% acetonitrile.

For liquid chromatography (LC) separation of the glycolysis/pentose phosphate pathway intermediates, an InfinityLab Poroshell 120 HILIC (2.7 μm, 150 by 2.1 mm, Agilent) was used flowing at 0.5 ml/min. The gradient of the mobile phases A (20 mM ammonium acetate [pH 9.8], 5% acetonitrile [ACN]) and B (100% acetonitrile) was as follows: 85% B for 1 min, to 40% B in 9 min, hold at 40% B for 2 min, then back to 85% B in 0.5 min. The liquid chromatography (LC) system was interfaced with a Sciex QTRAP 6500+ mass spectrometer equipped with a TurbolonSpray (TIS) electrospray ion source. Analyst software (version 1.6.3) was used to control sample acquisition and data analysis. The QTRAP 6500+ mass spectrometer was tuned and calibrated according to the manufacturer's recommendations. Metabolites were detected using MRM (multiple reaction monitoring) transitions that were previously optimized using standards. The instrument was set up to acquire in negative mode. For quantification, an external standard curve was prepared using a series of standard samples containing different concentrations of metabolites and fixed concentration of the internal standard. The limits of detection for glycolysis and pentose phosphate pathway intermediates were as follows: glucose 6-phosphate and glucose 1-phosphate/fructose 6-phosphate, 0.5 μM; glyceraldehyde 3-phosphate and ribulose 5-phosphate, 1 μM; erythrose-4-phosphate, 1.5 μM; pyruvate, 2/3-phosphoglycerate, phosphoenolpyruvate, and sedoheptulose-7-phosphate, 2 μM; fructose 1,6-bisphosphate, 3.9 μM. Resulting metabolite levels were normalized to parasitemia levels for each individual sample and reported as attogram per cell (ag/cell). Levels were averaged between three biological replicates and compared between control, FSM (5 μM for 24 h), and FTI (10 μM for 24 h).

SUPPLEMENTAL MATERIAL

Supplemental material is available online only.

FIG S1, JPG file, 2.2 MB.

FIG S2, JPG file, 0.7 MB.

FIG S3, JPG file, 0.7 MB.

FIG S4, JPG file, 1.8 MB.

FIG S5, JPG file, 0.7 MB.

FIG S6, JPG file, 0.5 MB.

TABLE S1, DOCX file, 0.01 MB.

TABLE S2, DOCX file, 0.01 MB.

ACKNOWLEDGMENTS

We thank Daniel Goldberg (Washington University) for supplying the anti-Exp-2 and anti-PM-V antibodies and Wesley Van Voorhis (University of Washington) for supplying BMS-388891. We thank Wandy Beatty (Washington University) for assistance with immuno-electron microscopy and Sophie Alvarez (University of Nebraska-Lincoln) for assistance with metabolomics profiling, and we are grateful for the assistance of the CHOP Proteomics Core facility. Research reported in this publication was supported by NIH/NIAID AI103280 (AOJ), AI123433 (AOJ), AI130584 (AOJ), AI144472 (AOJ), S10 RR026891, T32AI007172-37 (ESM), 1F32AI138373-01 (ESM), and T32GM007067 (AJJ). Audrey R. Odom John is an Investigator in the Pathogenesis of Infectious Diseases of the Burroughs Welcome Fund. We acknowledge support from the National Science Foundation under Grant number DBI-0922879 for acquisition of the LTQ-Velos Pro Orbitrap LC-MS/MS (Danforth Plant Sciences Center). We are grateful for the discussions and input from the members of the Odom John, Goldberg, and Adams laboratories.

REFERENCES

1. Shapiro LLM, Whitehead SA, Thomas MB. 2017. Quantifying the effects of temperature on mosquito and parasite traits that determine the transmission potential of human malaria. PLoS Biol 15:e2003489. https://doi.org/10.1371/journal.pbio.2003489.
2. Siau A, Silvie O, Franetich J-F, Yalaoui S, Marinach C, Hannoun L, van Gemert G-J, Luty AJF, Bischoff E, David PH, Snounou G, Vaquero C, Froissard P, Mazier D. 2008. Temperature shift and host cell contact up-regulate sporozoite expression of Plasmodium falciparum genes involved in hepatocyte infection. PLoS Pathog 4:e1000121. https://doi.org/10.1371/journal.ppat.1000121.
3. Kaiser K, Camargo N, Kappe SHI. 2003. Transformation of sporozoites into early exoerythrocytic malaria parasites does not require host cells. J Exp Med 197:1045–1050. https://doi.org/10.1084/jem.20022100.
4. Oakley MS, Gerald N, McCutchan TF, Aravind L, Kumar S. 2011. Clinical and molecular aspects of malaria fever. Trends Parasitol 27:442–449. https://doi.org/10.1016/j.pt.2011.06.004.
5. Gad A, Ali S, Zahoor T, Azarov N. 2018. Case report: a case of severe cerebral malaria managed with therapeutic hypothermia and other modalities for brain edema. Am J Trop Med Hyg 98:1120–1122. https://doi.org/10.4269/ajtmh.17-0794.
6. Rehman K, Sauerzopf U, Veletzky L, Lötsch F, Groger M, Ramharter M. 2016. Effect of mild medical hypothermia on in vitro growth of *Plasmodium falciparum* and the activity of anti-malarial drugs. Malar J 15:162. https://doi.org/10.1186/s12936-016-1215-8.
7. Rojas MO, Wasserman M. 1993. Effect of low temperature on the in vitro growth of Plasmodium falciparum. J Eukaryot Microbiol 40:149–152. https://doi.org/10.1111/j.1550-7408.1993.tb04895.x.
8. Henrici RC, van Schalkwyk DA, Sutherland CJ. 2019. Transient temperature fluctuations severely decrease P. falciparum susceptibility to artemisinin in vitro. Int J Parasitol Drugs Drug Resist 9:23–26. https://doi.org/10.1016/j.ijpddr.2018.12.003.
9. Huang F, Takala-Harrison S, Jacob CG, Liu H, Sun X, Yang H, Nyunt MM, Adams M, Zhou S, Xia Z, Ringwald P, Bustos MD, Tang L, Plowe CV. 2015. A single mutation in K13 predominates in southern China and is associated with delayed clearance of Plasmodium falciparum following artemisinin treatment. J Infect Dis 212:1629–1635. https://doi.org/10.1093/infdis/jiv249.
10. Amaratunga C, Sreng S, Suon S, Phelps ES, Stepniewska K, Lim P, Zhou C, Mao S, Anderson JM, Lindegardh N, Jiang H, Song J, Su X-z, White NJ, Dondorp AM, Anderson TJC, Fay MP, Mu J, Duong S, Fairhurst RM. 2012. Artemisinin-resistant Plasmodium falciparum in Pursat province, western Cambodia: a parasite clearance rate study. Lancet Infect Dis 12:851–858. https://doi.org/10.1016/S1473-3099(12)70181-0.
11. Phyo AP, Nkhoma S, Stepniewska K, Ashley EA, Nair S, McGready R, Ler Moo C, Al-Saai S, Dondorp AM, Lwin KM, Singhasivanon P, Day NP, White NJ, Anderson TJ, Nosten F. 2012. Emergence of artemisinin-resistant malaria on the western border of Thailand: a longitudinal study. Lancet 379:1960–1966. https://doi.org/10.1016/S0140-6736(12)60484-X.
12. Dondorp AM, Nosten F, Yi P, Das D, Phyo AP, Tarning J, Lwin KM, Ariey F, Hanpithakpong W, Lee SJ, Ringwald P, Silamut K, Imwong M, Chotivanich K, Lim P, Herdman T, An SS, Yeung S, Singhasivanon P, Day NPJ, Lindegardh N, Socheat D, White NJ. 2009. Artemisinin resistance in Plasmodium falciparum malaria. N Engl J Med 361:455–467. https://doi.org/10.1056/NEJMoa0808859.
13. Thriemer K, Hong NV, Rosanas-Urgell A, Phuc BQ, Ha DM, Pockele E, Guetens P, Van NV, Duong TT, Amambua-Ngwa A, D'Alessandro U, Erhart A. 2014. Delayed parasite clearance after treatment with dihydroartemisinin-piperaquine in Plasmodium falciparum malaria patients in central Vietnam. Antimicrob Agents Chemother 58:7049–7055. https://doi.org/10.1128/AAC.02746-14.
14. Amato R, Miotto O, Woodrow CJ, Almagro-Garcia J, Sinha I, Campino S, Mead D, Drury E, Kekre M, Sanders M, Amambua-Ngwa A, Amaratunga C, Amenga-Etego L, Andrianaranjaka V, Apinjoh T, Ashley E, Auburn S, Awandare GA, Baraka V, Barry A, Boni MF, Borrmann S, Bousema T, Branch O, Bull PC, Chotivanich K, Conway DJ, Craig A, Day NP, Djimdé A, Dolecek C, Dondorp AM, Drakeley C, Duffy P, Echeverry DF, Egwang TG, Fairhurst RM, Faiz MA, Fanello CI, Hien TT, Hodgson A, Imwong M, Ishengoma D, Lim P, Lon C, Marfurt J, Marsh K, Mayxay M, Michon P, Mobegi V, Mokuolu OA, et al. 2016. Genomic epidemiology of artemisinin resistant malaria. Elife 5:e08714. https://doi.org/10.7554/eLife.08714.
15. Kyaw MP, Nyunt MH, Chit K, Aye MM, Aye KH, Aye MM, Lindegardh N, Tarning J, Imwong M, Jacob CG, Rasmussen C, Perin J, Ringwald P, Nyunt MM. 2013. Reduced susceptibility of Plasmodium falciparum to artesunate in southern Myanmar. PLoS One 8:e57689. https://doi.org/10.1371/journal.pone.0057689.

16. Hien TT, Thuy-Nhien NT, Phu NH, Boni MF, Thanh NV, Nha-Ca NT, Thai LH, Thai CQ, Toi PV, Thuan PD, Long LT, Dong LT, Merson L, Dolecek C, Stepniewska K, Ringwald P, White NJ, Farrar J, Wolbers M. 2012. In vivo susceptibility of Plasmodium falciparum to artesunate in Binh Phuoc Province, Vietnam. Malar J 11:355. https://doi.org/10.1186/1475-2875-11-355.
17. Leang R, Taylor WRJ, Bouth DM, Song L, Tarning J, Char MC, Kim S, Witkowski B, Duru V, Domergue A, Khim N, Ringwald P, Menard D. 2015. Evidence of Plasmodium falciparum malaria multidrug resistance to artemisinin and piperaquine in western Cambodia: dihydroartemisinin-piperaquine open-label multicenter clinical assessment. Antimicrob Agents Chemother 59:4719–4726. https://doi.org/10.1128/AAC.00835-15.
18. Jomaa H, Wiesner J, Sanderbrand S, Altincicek B, Weidemeyer C, Hintz M, Türbachova I, Eberl M, Zeidler J, Lichtenthaler HK, Soldati D, Beck E. 1999. Inhibitors of the nonmevalonate pathway of isoprenoid biosynthesis as antimalarial drugs. Science 285:1573–1576. https://doi.org/10.1126/science.285.5433.1573.
19. Cassera MB, Gozzo FC, D'Alexandri FL, Merino EF, del Portillo HA, Peres VJ, Almeida IC, Eberlin MN, Wunderlich G, Wiesner J, Jomaa H, Kimura EA, Katzin AM. 2004. The methylerythritol phosphate pathway is functionally active in all intraerythrocytic stages of Plasmodium falciparum. J Biol Chem 279:51749–51759. https://doi.org/10.1074/jbc.M408360200.
20. Odom AR, Van Voorhis WC. 2010. Functional genetic analysis of the Plasmodium falciparum deoxyxylulose 5-phosphate reductoisomerase gene. Mol Biochem Parasitol 170:108–111. https://doi.org/10.1016/j.molbiopara.2009.12.001.
21. Zhang B, Watts KM, Hodge D, Kemp LM, Hunstad DA, Hicks LM, Odom AR. 2011. A second target of the antimalarial and antibacterial agent fosmidomycin revealed by cellular metabolic profiling. Biochemistry 50:3570–3577. https://doi.org/10.1021/bi200113y.
22. Yeh E, DeRisi JL. 2011. Chemical rescue of malaria parasites lacking an apicoplast defines organelle function in blood-stage Plasmodium falciparum. PLoS Biol 9:e1001138. https://doi.org/10.1371/journal.pbio.1001138.
23. Howe R, Kelly M, Jimah J, Hodge D, Odom AR. 2013. Isoprenoid biosynthesis inhibition disrupts Rab5 localization and food vacuolar integrity in Plasmodium falciparum. Eukaryot Cell 12:215–223. https://doi.org/10.1128/EC.00073-12.
24. Buckner FS, Eastman RT, Yokoyama K, Gelb MH, Van Voorhis WC. 2005. Protein farnesyl transferase inhibitors for the treatment of malaria and African trypanosomiasis. Curr Opin Investig Drugs 6:791–797.
25. Glenn MP, Chang S-Y, Hucke O, Verlinde CLMJ, Rivas K, Hornéy C, Yokoyama K, Buckner FS, Pendyala PR, Chakrabarti D, Gelb M, Van Voorhis WC, Sebti SM, Hamilton AD. 2005. Structurally simple farnesyltransferase inhibitors arrest the growth of malaria parasites. Angew Chem Int Ed Engl 44:4903–4906. https://doi.org/10.1002/anie.200500674.
26. Glenn MP, Chang S-Y, Hornéy C, Rivas K, Yokoyama K, Pusateri EE, Fletcher S, Cummings CG, Buckner FS, Pendyala PR, Chakrabarti D, Sebti SM, Gelb M, Van Voorhis WC, Hamilton AD. 2006. Structurally simple, potent, Plasmodium selective farnesyltransferase inhibitors that arrest the growth of malaria parasites. J Med Chem 49:5710–5727. https://doi.org/10.1021/jm060081v.
27. Nallan L, Bauer KD, Bendale P, Rivas K, Yokoyama K, Hornéy CP, Pendyala PR, Floyd D, Lombardo LJ, Williams DK, Hamilton A, Sebti S, Windsor WT, Weber PC, Buckner FS, Chakrabarti D, Gelb MH, Van Voorhis WC. 2005. Protein farnesyltransferase inhibitors exhibit potent antimalarial activity. J Med Chem 48:3704–3713. https://doi.org/10.1021/jm0491039.
28. Chakrabarti D, Da Silva T, Barger J, Paquette S, Patel H, Patterson S, Allen CM. 2002. Protein farnesyltransferase and protein prenylation in Plasmodium falciparum. J Biol Chem 277:42066–42073. https://doi.org/10.1074/jbc.M202860200.
29. Chakrabarti D, Azam T, DelVecchio C, Qiu L, Park YI, Allen CM. 1998. Protein prenyl transferase activities of Plasmodium falciparum. Mol Biochem Parasitol 94:175–184. https://doi.org/10.1016/s0166-6851(98)00065-6.
30. Suazo KF, Schaber C, Palsuledesai CC, Odom John AR, Distefano MD. 2016. Global proteomic analysis of prenylated proteins in Plasmodium falciparum using an alkyne-modified isoprenoid analogue. Sci Rep 6:38615. https://doi.org/10.1038/srep38615.
31. Gisselberg JE, Zhang L, Elias JE, Yeh E. 2017. The prenylated proteome of Plasmodium falciparum reveals pathogen-specific prenylation activity and drug mechanism-of-action. Mol Cell Proteomics 16:S54–S64. https://doi.org/10.1074/mcp.M116.064550.
32. Lu K-Y, Pasaje CFA, Srivastava T, Loiselle DR, Niles JC, Derbyshire E. 2020. Phosphatidylinositol 3-phosphate and Hsp70 protect Plasmodium falciparum from heat-induced cell death. Elife 9 https://doi.org/10.7554/eLife.56773.
33. Acharya P, Kumar R, Tatu U. 2007. Chaperoning a cellular upheaval in malaria: heat shock proteins in Plasmodium falciparum. Mol Biochem Parasitol 153:85–94. https://doi.org/10.1016/j.molbiopara.2007.01.009.
34. Njunge JM, Ludewig MH, Boshoff A, Pesce E-R, Blatch GL. 2013. Hsp70s and J proteins of Plasmodium parasites infecting rodents and primates: structure, function, clinical relevance, and drug targets. Curr Pharm Des 19:387–403. https://doi.org/10.2174/138161213804143734.
35. Botha M, Pesce ER, Blatch GL. 2007. The Hsp40 proteins of Plasmodium falciparum and other apicomplexa: regulating chaperone power in the parasite and the host. Int J Biochem Cell Biol 39:1781–1803. https://doi.org/10.1016/j.biocel.2007.02.011.
36. Botha M, Chiang AN, Needham PG, Stephens LL, Hoppe HC, Külzer S, Przyborski JM, Lingelbach K, Wipf P, Brodsky JL, Shonhai A, Blatch GL. 2011. Plasmodium falciparum encodes a single cytosolic type i Hsp40 that functionally interacts with Hsp70 and is upregulated by heat shock. Cell Stress Chaperones 16:389–401. https://doi.org/10.1007/s12192-010-0250-6.
37. Caplan AJ, Tsai J, Casey PJ, Douglas MG. 1992. Farnesylation of YDJ1p is required for function at elevated growth temperatures in Saccharomyces cerevisiae. J Biol Chem 267:18890–18895. https://doi.org/10.1016/S0021-9258(19)37044-9.
38. Flom GA, Lemieszek M, Fortunato EA, Johnson JL. 2008. Farnesylation of Ydj1 is required for in vivo interaction with Hsp90 client proteins. MBoC 19:5249–5258. https://doi.org/10.1091/mbc.e08-04-0435.
39. Hildebrandt ER, Cheng M, Zhao P, Kim JH, Wells L, Schmidt WK. 2016. A shunt pathway limits the CaaX processing of Hsp40 Ydj1p and regulates Ydj1p-dependent phenotypes. Elife 5:e15899. https://doi.org/10.7554/eLife.15899.
40. Sharma YD. 1992. Structure and possible function of heat-shock proteins in Falciparum malaria. Comp Biochem Physiol B 102:437–444. https://doi.org/10.1016/0305-0491(92)90033-N.
41. Pavithra SR, Banumathy G, Joy O, Singh V, Tatu U. 2004. Recurrent fever promotes Plasmodium falciparum development in human erythrocytes. J Biol Chem 279:46692–46699. https://doi.org/10.1074/jbc.M409165200.
42. Banumathy G, Singh V, Pavithra SR, Tatu U. 2003. Heat shock protein 90 function is essential for Plasmodium falciparum growth in human erythrocytes. J Biol Chem 278:18336–18345. https://doi.org/10.1074/jbc.M211309200.
43. Muralidharan V, Oksman A, Pal P, Lindquist S, Goldberg DE. 2012. Plasmodium falciparum heat shock protein 110 stabilizes the asparagine repeat-rich parasite proteome during malarial fevers. Nat Commun 3:1310. https://doi.org/10.1038/ncomms2306.
44. Eastman RT, White J, Hucke O, Bauer K, Yokoyama K, Nallan L, Chakrabarti D, Verlinde CLMJ, Gelb MH, Rathod PK, Van Voorhis WC. 2005. Resistance to a protein farnesyltransferase inhibitor in Plasmodium falciparum. J Biol Chem 280:13554–13559. https://doi.org/10.1074/jbc.M413556200.
45. Zhang M, Wang C, Otto TD, Oberstaller J, Liao X, Adapa SR, Udenze K, Bronner IF, Casandra D, Mayho M, Brown J, Li S, Swanson J, Rayner JC, Jiang RHY, Adams JH. 2018. Uncovering the essential genes of the human malaria parasite Plasmodium falciparum by saturation mutagenesis. Science 360:eaap7847. https://doi.org/10.1126/science.aap7847.
46. Imlay LS, Armstrong CM, Masters MC, Li T, Price KE, Edwards RL, Mann KM, Li LX, Stallings CL, Berry NG, O'Neill PM, Odom AR. 2015. Plasmodium IspD (2-C-methyl-D-erythritol 4-phosphate cytidyltransferase), an essential and druggable antimalarial target. ACS Infect Dis 1:157–167. https://doi.org/10.1021/id500047s.
47. Shonhai A, Maier AG, Przyborski JM, Blatch GL. 2011. Intracellular protozoan parasites of humans: the role of molecular chaperones in development and pathogenesis. Protein Pept Lett 18:143–157. https://doi.org/10.2174/092986611794475002.
48. Shonhai A, Boshoff A, Blatch GL. 2005. Plasmodium falciparum heat shock protein 70 is able to suppress the thermosensitivity of an Escherichia coli DnaK mutant strain. Mol Genet Genomics 274:70–78. https://doi.org/10.1007/s00438-005-1150-9.
49. Shonhai A, Boshoff A, Blatch GL. 2007. The structural and functional diversity of Hsp70 proteins from Plasmodium falciparum. Protein Sci 16:1803–1818. https://doi.org/10.1110/ps.072918107.
50. Matambo TS, Odunuga OO, Boshoff A, Blatch GL. 2004. Overproduction, purification, and characterization of the Plasmodium falciparum heat shock protein 70. Protein Expr Purif 33:214–222. https://doi.org/10.1016/j.pep.2003.09.010.
51. Kelley WL. 1998. The J-domain family and the recruitment of chaperone power. Trends Biochem Sci 23:222–227. https://doi.org/10.1016/S0968-0004(98)01215-8.
52. Feldman DE, Frydman J. 2000. Protein folding in vivo: the importance of molecular chaperones. Curr Opin Struct Biol 10:26–33. https://doi.org/10.1016/S0959-440X(99)00044-5.
53. Wittung-Stafshede P, Guidry J, Horne BE, Landry SJ. 2003. The J-domain of Hsp40 couples ATP hydrolysis to substrate capture in Hsp70. Biochemistry 42:4937–4944. https://doi.org/10.1021/bi027333o.

54. Hennessy F, Cheetham ME, Dirr HW, Blatch GL. 2000. Analysis of the levels of conservation of the J domain among the various types of DnaJ-like proteins. Cell Stress Chaper 5:347–358. https://doi.org/10.1379/1466-1268(2000)005<0347:AOTLOC>2.0.CO;2.
55. Tsai J, Douglas MG. 1996. A conserved HPD sequence of the J-domain is necessary for YDJ1 stimulation of Hsp70 ATPase activity at a site distinct from substrate binding. J Biol Chem 271:9347–9354. https://doi.org/10.1074/jbc.271.16.9347.
56. Beck JR, Muralidharan V, Oksman A, Goldberg DE. 2014. PTEX component HSP101 mediates export of diverse malaria effectors into host erythrocytes. Nature 511:592–595. https://doi.org/10.1038/nature13574.
57. Elsworth B, Matthews K, Nie CQ, Kalanon M, Charnaud SC, Sanders PR, Chisholm SA, Counihan NA, Shaw PJ, Pino P, Chan J-A, Azevedo MF, Rogerson SJ, Beeson JG, Crabb BS, Gilson PR, de Koning-Ward TF. 2014. PTEX is an essential nexus for protein export in malaria parasites. Nature 511:587–591. https://doi.org/10.1038/nature13555.
58. Acharya P, Chaubey S, Grover M, Tatu U, Cowman A. 2012. An exported heat shock protein 40 associates with pathogenesis-related knobs in Plasmodium falciparum infected erythrocytes. PLoS One 7:e44605. https://doi.org/10.1371/journal.pone.0044605.
59. Hanker AB, Mitin N, Wilder RS, Henske EP, Tamanoi F, Cox AD, Der CJ. 2010. Differential requirement of CAAX-mediated posttranslational processing for Rheb localization and signaling. Oncogene 29:380–391. https://doi.org/10.1038/onc.2009.336.
60. Buerger C, DeVries B, Stambolic V. 2006. Localization of Rheb to the endomembrane is critical for its signaling function. Biochem Biophys Res Commun 344:869–880. https://doi.org/10.1016/j.bbrc.2006.03.220.
61. Noiva R. 1999. Protein disulfide isomerase: the multifunctional redox chaperone of the endoplasmic reticulum. Semin Cell Dev Biol 10:481–493. https://doi.org/10.1006/scdb.1999.0319.
62. Mouray E, Moutiez M, Girault S, Sergheraert C, Florent I, Grellier P. 2007. Biochemical properties and cellular localization of Plasmodium falciparum protein disulfide isomerase. Biochimie 89:337–346. https://doi.org/10.1016/j.biochi.2006.11.001.
63. Jones ML, Collins MO, Goulding D, Choudhary JS, Rayner JC. 2012. Analysis of protein palmitoylation reveals a pervasive role in Plasmodium development and pathogenesis. Cell Host Microbe 12:246–258. https://doi.org/10.1016/j.chom.2012.06.005.
64. Resh MD. 2006. Use of analogs and inhibitors to study the functional significance of protein palmitoylation. Methods 40:191–197. https://doi.org/10.1016/j.ymeth.2006.04.013.
65. Choy E, Chiu VK, Silletti J, Feoktistov M, Morimoto T, Michaelson D, Ivanov IE, Philips MR. 1999. Endomembrane trafficking of ras: the CAAX motif targets proteins to the ER and Golgi. Cell 98:69–80. https://doi.org/10.1016/S0092-8674(00)80607-8.
66. Daubenberger CA, Tisdale EJ, Curcic M, Diaz D, Silvie O, Mazier D, Eling W, Bohrmann B, Matile H, Pluschke G. 2003. The N′-terminal domain of glyceraldehyde-3-phosphate dehydrogenase of the apicomplexan Plasmodium falciparum mediates GTPase Rab2-dependent recruitment to membranes. Biol Chem 384:1227–1237.
67. Sangolgi PB, Balaji C, Dutta S, Jindal N, Jarori GK. 2016. Cloning, expression, purification and characterization of Plasmodium spp. glyceraldehyde-3-phosphate dehydrogenase. Protein Expr Purif 117:17–25. https://doi.org/10.1016/j.pep.2015.08.028.
68. Zhang M, Wang C, Oberstaller J, Thomas P, Otto TD, Casandra D, Boyapalle S, Adapa SR, Xu S, Button-Simons K, Mayho M, Rayner JC, Ferdig MT, Jiang RHY, Adams JH. 2020. The endosymbiotic origins of the apicoplast link fever-survival and artemisinin-resistance in the malaria parasite. bioRxiv https://doi.org/10.1101/2020.12.10.419788.
69. Redd SC, Luby SP, Hightower AW, Kazembe PN, Nwanyanwu O, Ziba C, Chitsulo L, Franco C, Olivar M, Wirima JJ. 1996. Clinical algorithm for treatment of Plasmodium falciparum malaria in children. Lancet 347:223–227. https://doi.org/10.1016/S0140-6736(96)90404-3.
70. Kennedy K, Cobbold SA, Hanssen E, Birnbaum J, Spillman NJ, McHugh E, Brown H, Tilley L, Spielmann T, McConville MJ, Ralph SA. 2019. Delayed death in the malaria parasite Plasmodium falciparum is caused by disruption of prenylation-dependent intracellular trafficking. PLoS Biol 17:e3000376. https://doi.org/10.1371/journal.pbio.3000376.
71. Rocks O, Peyker A, Kahms M, Verveer PJ, Koerner C, Lumbierres M, Kuhlmann J, Waldmann H, Wittinghofer A, Bastiaens PIH. 2005. An acylation cycle regulates localization and activity of palmitoylated Ras isoforms. Science 307:1746–1752. https://doi.org/10.1126/science.1105654.
72. Pesce E-R, Maier AG, Blatch GL. 2014. Role of the Hsp40 family of proteins in the survival and pathogenesis of the malaria parasite, p 71–85. In Shonhai A, Blatch GL (ed), Heat shock proteins of malaria. Springer, Netherlands. https://doi.org/10.1007/978-94-007-7438-4_4.
73. Kanazawa M, Terada K, Kato S, Mori M. 1997. HSDJ, a human homolog of DnaJ, is farnesylated and is involved in protein import into mitochondria. J Biochem 121:890–895. https://doi.org/10.1093/oxfordjournals.jbchem.a021670.
74. Barghetti A, Sjögren L, Floris M, Paredes EB, Wenkel S, Brodersen P. 2017. Heat-shock protein 40 is the key farnesylation target in meristem size control, abscisic acid signaling, and drought resistance. Genes Dev 31:2282–2295. https://doi.org/10.1101/gad.301242.117.
75. Zhu JK, Bressan RA, Hasegawa PM. 1993. Isoprenylation of the plant molecular chaperone ANJ1 facilitates membrane association and function at high temperature. Proc Natl Acad Sci U S A 90:8557–8561. https://doi.org/10.1073/pnas.90.18.8557.
76. Wu J-R, Wang T-Y, Weng C-P, Duong NKT, Wu S-J. 2019. AtJ3, a specific HSP40 protein, mediates protein farnesylation-dependent response to heat stress in Arabidopsis. Planta 250:1449–1460. https://doi.org/10.1007/s00425-019-03239-7.
77. Wu J-R, Wang L-C, Lin Y-R, Weng C-P, Yeh C-H, Wu S-J. 2017. The Arabidopsis heat-intolerant 5 (hit5)/enhanced response to aba 1 (era1) mutant reveals the crucial role of protein farnesylation in plant responses to heat stress. New Phytol 213:1181–1193. https://doi.org/10.1111/nph.14212.
78. Pesce E-R, Blatch GL, Edkins AL. 2016. Hsp40 co-chaperones as drug targets: towards the development of specific inhibitors, p 163–195. In McAlpine SR, Edkins AL (ed), Heat shock protein inhibitors: success stories. Springer International Publishing. https://doi.org/10.1007/7355_2015_92.
79. Daniyan MO, Blatch GL. 2017. Plasmodial Hsp40s: new avenues for antimalarial drug discovery. Curr Pharm Des 23:4555–4570. https://doi.org/10.2174/1381612823666170124142439.
80. Cerqueira GC, Cheeseman IH, Schaffner SF, Nair S, McDew-White M, Phyo AP, Ashley EA, Melnikov A, Rogov P, Birren BW, Nosten F, Anderson TJC, Neafsey DE. 2017. Longitudinal genomic surveillance of Plasmodium falciparum malaria parasites reveals complex genomic architecture of emerging artemisinin resistance. Genome Biol 18:78. https://doi.org/10.1186/s13059-017-1204-4.
81. Guggisberg AM, Park J, Edwards RL, Kelly ML, Hodge DM, Tolia NH, Odom AR. 2014. A sugar phosphatase regulates the methylerythritol phosphate (MEP) pathway in malaria parasites. Nat Commun 5:4467. https://doi.org/10.1038/ncomms5467.
82. Banerjee R, Liu J, Beatty W, Pelosof L, Klemba M, Goldberg DE. 2002. Four plasmepsins are active in the Plasmodium falciparum food vacuole, including a protease with an active-site histidine. Proc Natl Acad Sci U S A 99:990–995. https://doi.org/10.1073/pnas.022630099.
83. Hall R, McBride J, Morgan G, Tait A, Zolg JW, Walliker D, Scaife J. 1983. Antigens of the erythrocytic stages of the human malaria parasite Plasmodium falciparum detected by monoclonal antibodies. Mol Biochem Parasitol 7:247–265. https://doi.org/10.1016/0166-6851(83)90025-7.
84. Broom BM, Ryan MC, Brown RE, Ikeda F, Stucky M, Kane DW, Melott J, Wakefield C, Casasent TD, Akbani R, Weinstein JN. 2017. A galaxy implementation of next-generation clustered heatmaps for interactive exploration of molecular profiling data. Cancer Res 77:e23–e26. https://doi.org/10.1158/0008-5472.CAN-17-0318.
85. Ashburner M, Ball CA, Blake JA, Botstein D, Butler H, Cherry JM, Davis AP, Dolinski K, Dwight SS, Eppig JT, Harris MA, Hill DP, Issel-Tarver L, Kasarskis A, Lewis S, Matese JC, Richardson JE, Ringwald M, Rubin GM, Sherlock G, The Gene Ontology Consortium. 2000. Gene ontology: tool for the unification of biology. Nat Genet 25:25–29. https://doi.org/10.1038/75556.
86. 2021. The Gene Ontology resource: enriching a GOld mine. Nucleic Acids Res 49:D325–D334.